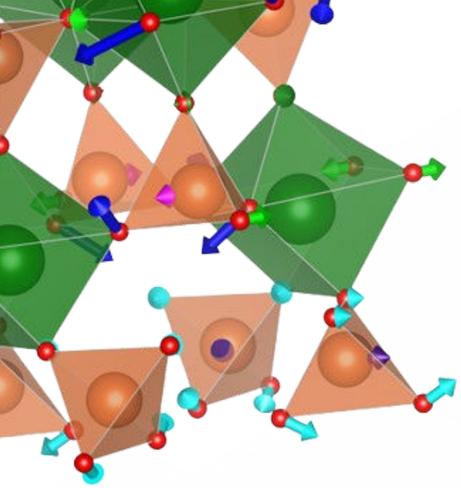

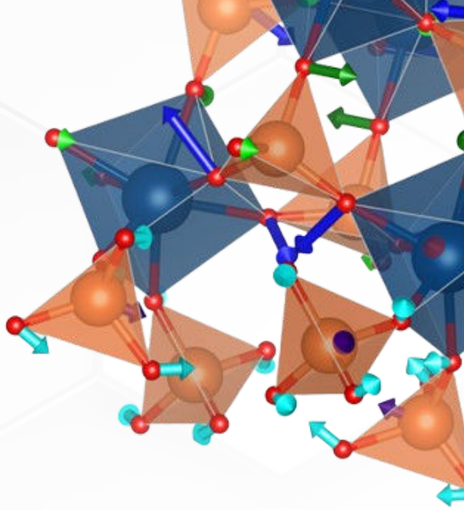

Universidad de La Laguna

Faculty of Sciences

Structural Mechanisms of Ferroelectricity and Ferroelasticity in Compounds with the Formula: β′-$RE_2(MoO_4)_3$

Physics Final Degree Project

Alberto Reyes Castro

July 2025

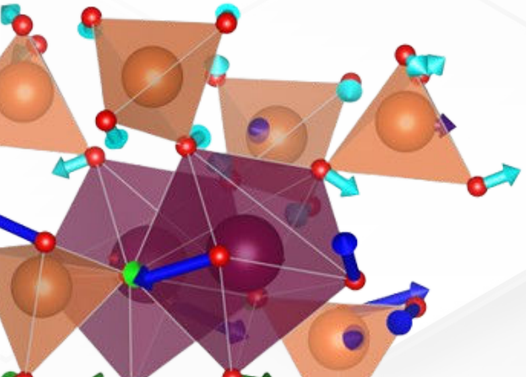

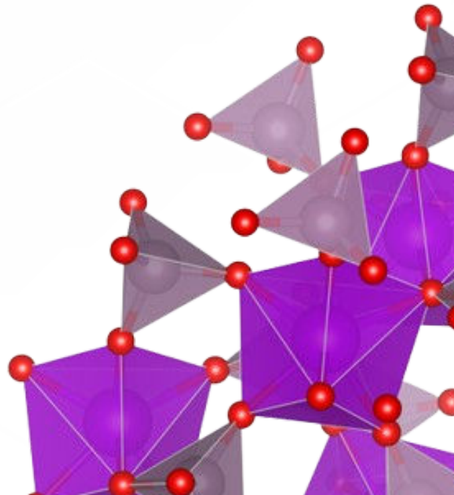

Contents

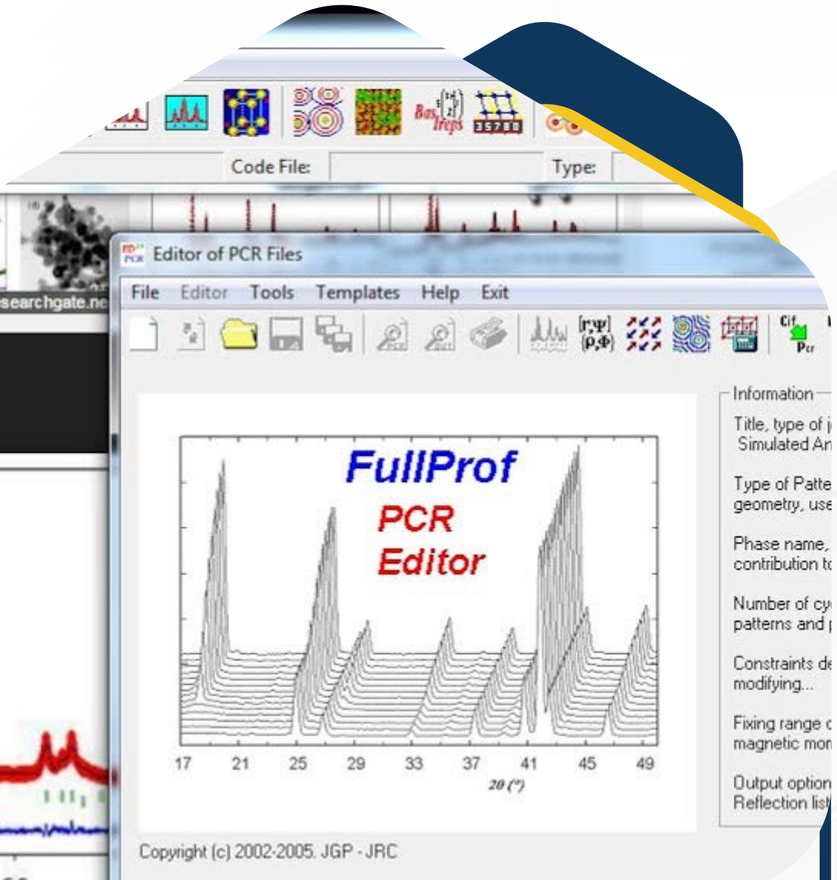

01 **Introduction**

1. What are ferroic materials?

- **Definition:** Materials exhibiting a spontaneous, switchable order parameter (magnetization, polarization, or strain) in response to external stimuli.

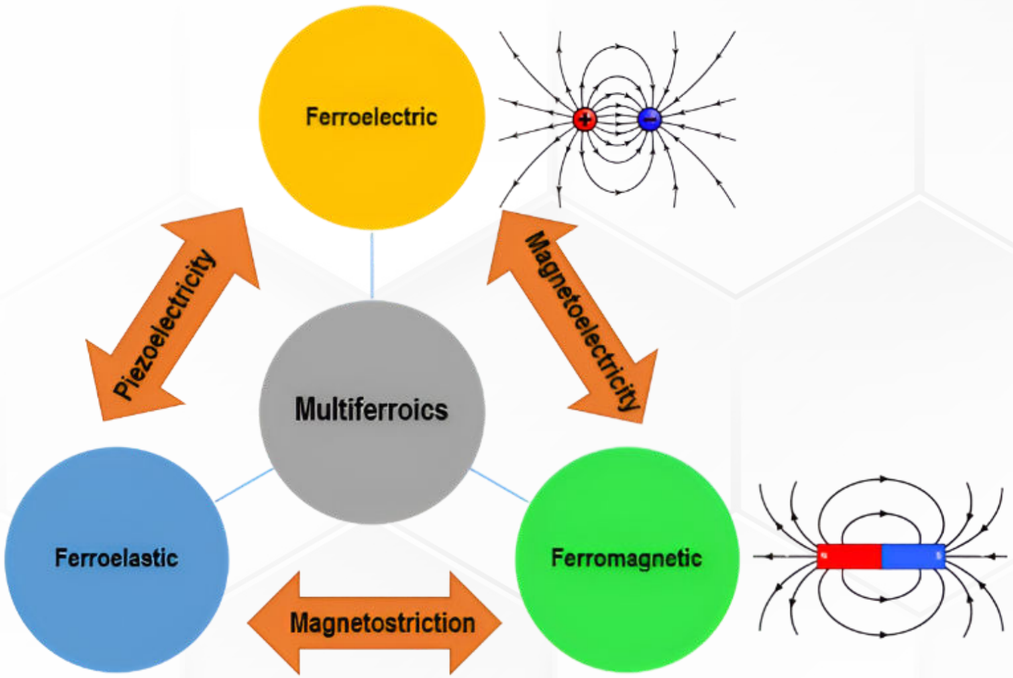

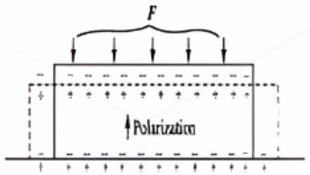

- **Classes:**
  - **Ferromagnets:** spontaneous magnetization
  - **Ferroelectrics:** reversible electric polarization
  - **Ferroelastics:** switchable mechanical strain

- **Multiferroics:** Compounds combining two or more ferroic orderings for multifunctional devices.

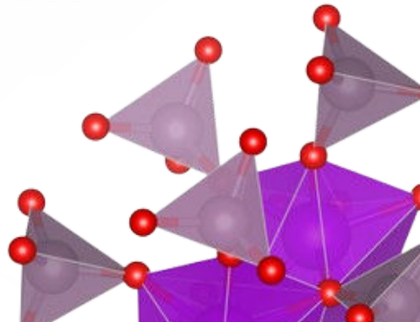

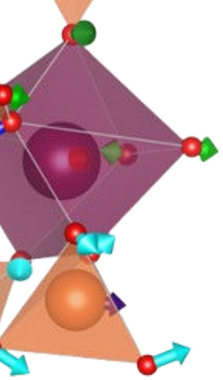

01 **Introduction**

2. Ferroelastics, Ferroelectrics, β′-$RE_2(MoO_4)_3$ Compounds and its Phase transitions

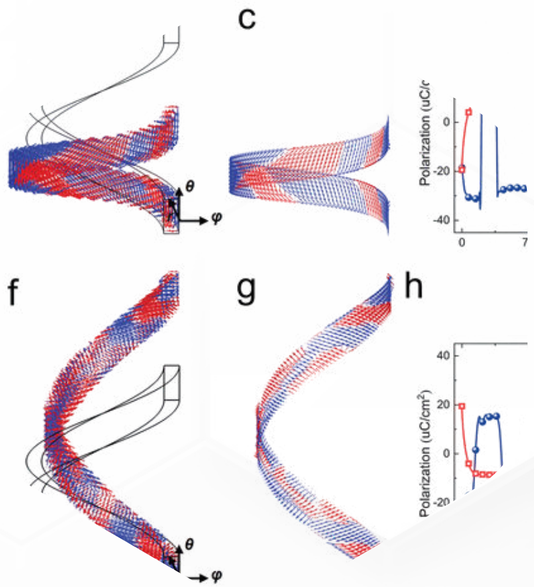

- **Ferroelectrics:**
  - Require non-centrosymmetric, polar axis
  - Exhibit domains & hysteresis under cyclic fields
  - Key for memory, piezoelectric, pyroelectric, capacitors
- **Ferroelastics:**
  - Shape reoriented by stress, reversible domain switching
  - Used in shape-memory, stress sensors, soft robotics

- **Material Family: $RE_2(MoO_4)_3$, where RE = Rare-Earth element**
  - Four polymorphs Phases: α, β, β′, and γ
  - Phase stability depends on lantanic ionic radius, T, P, and synthesis conditions
  - Structural diversity yields functional properties in optoelectronics and ferroics
  - First synthesized (La, Pr, Nd) by Hitchcock in 1895

3. Research context, Motivations and Objectives

Objectives:

- Perform Rietveld refinements and AMPLIMODES analysis on X-ray and neutron data
- Differentiate primary (M2M4) and secondary (GM3) order parameters
- Compare RE/Mo vs. O displacements and contrast chemical substitution (ionic radius) with hydrostatic pressure
- Deepen expertise in crystallography, solid-state physics, and diffraction techniques

- **Current focus: β → β′ structural transition in Tb, Dy & Ho trimolybdates**

Research Context:

- Previous CCDD Studies include thermal expansion, transport mechanisms, pressure effects, and luminescence

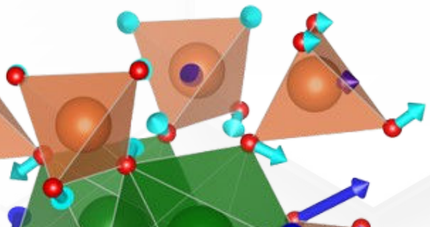

01 **Introduction**

3. Research context, Motivations and Objectives

Motivations:

Elements of the rare-earth series RE are shown:

Blocks with arrowheads: Ferroelectric β’ compounds.
Arrow size is proportional to the polarization attributed to β’-$RE_2(MoO_4)_3$ members.
Polarization ↓ as ionic radius ↓
Blocks without arrows: Non-ferroelectric (or with other structures).
Pm excluded due to radioactivity.

Hysteresis loops (polarization vs electric field) measured by the CCDD group

Three compositions of the solid solution **$La_{2-x}Er_x(MoO_4)_3$**:
x = 0.75 → red arrow, x = 1 → fuchsia arrow, x = 1.25 → violet arrow
The opposite trend occurs: **Polarization ↑ as ionic radius ↓ (↑ Er) → stronger ferroelectric character**
These compositions show significantly higher polarizations than classical molybdates

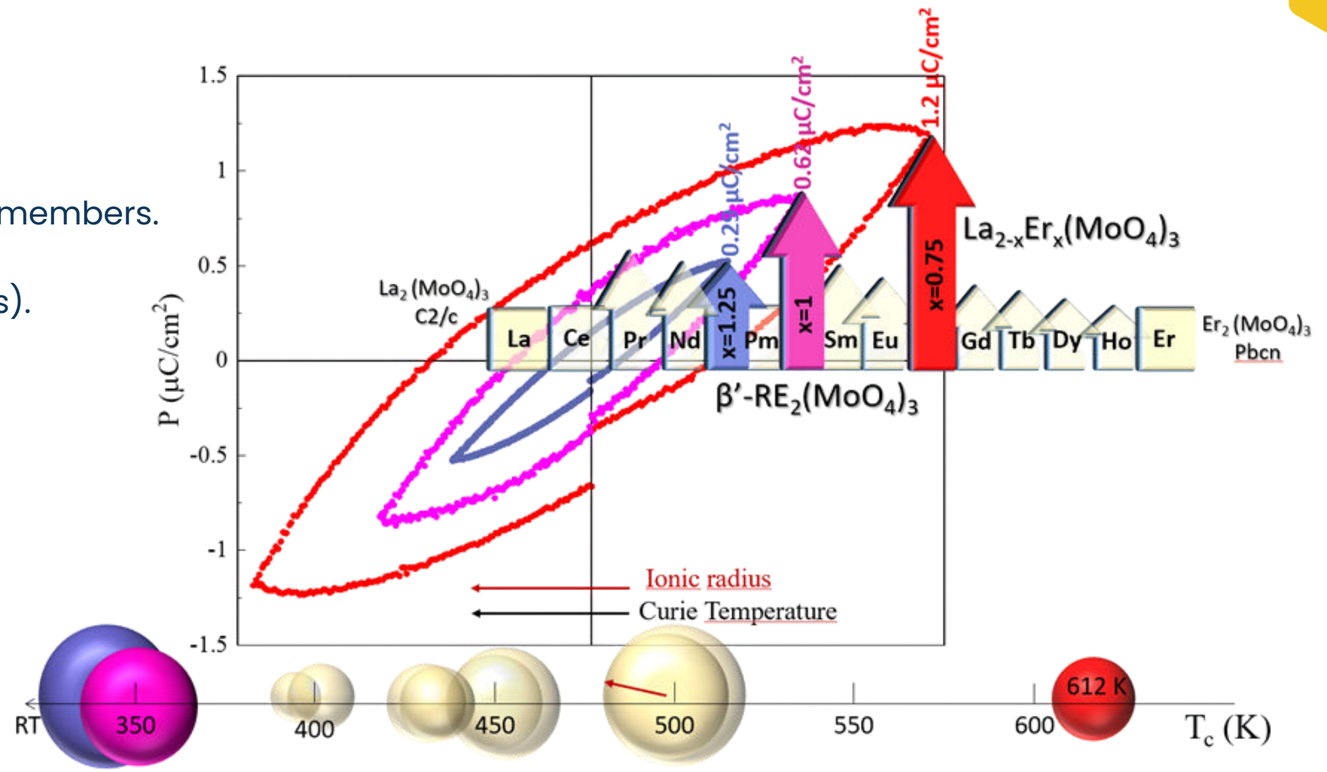

Bottom row: Ionic radius and Curie temperature (Tc)

Colorless spheres → size proportional to the ionic radius of RE^{3+}, placed at their corresponding Tc.

Trends:
In classical molybdates: ↑ ionic radius → ↑ Tc
In $La_{2-x}Er_x(MoO_4)_3$: Opposite trend → ↓ ionic radius → ↑ Tc
This justifies a systematic study of ferroelectricity in conventional molybdates, where existing data are outdated and fragmented.

4. Fundamentals of Symmetry and Crystallography for Structural Analysis

Direct Lattice & Symmetry Elements:

- Crystal defined by basis vectors a, b, c generating a 3D periodic lattice
- Primitive vs Centered cells; symmetry ops include rotations, reflections, inversions, screw axes, glide planes

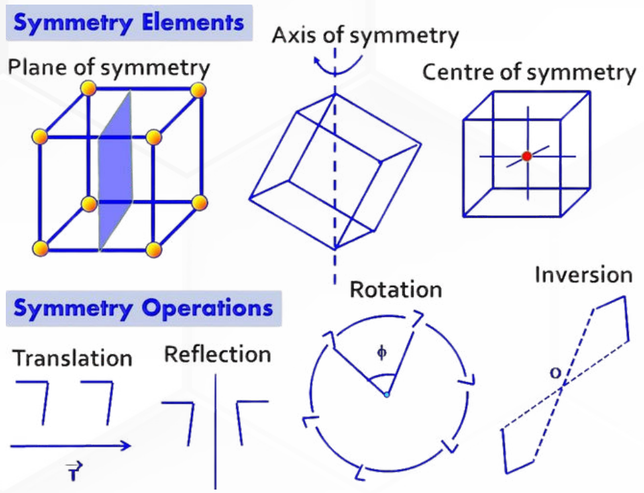

Point Groups & Space Groups:

- 32 point groups in 7 crystal systems → 14 Bravais lattices
- 230 **space groups** combine point and translational symmetries
- Wyckoff positions describe atomic sites and multiplicities

Reciprocal Lattice & Diffraction

- Miller indices (hkl) label plane families; **vector G_{hkl} = h a* + k b* + l c***
- **Bragg's law** ($n\lambda = 2 d_{hkl} \sin\theta$) ↔ Laue condition ($k - k_0 = G_{hkl}$)
- First Brillouin zone defines allowed k-states for waves in crystals

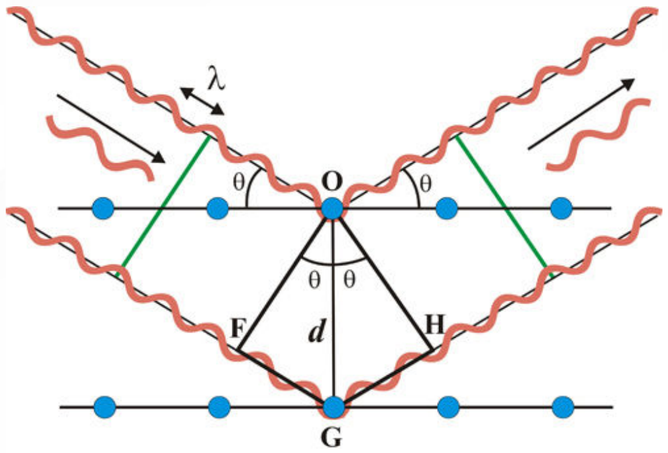

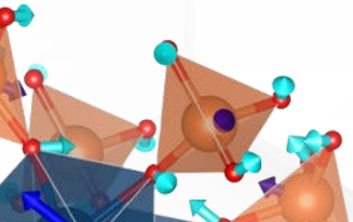

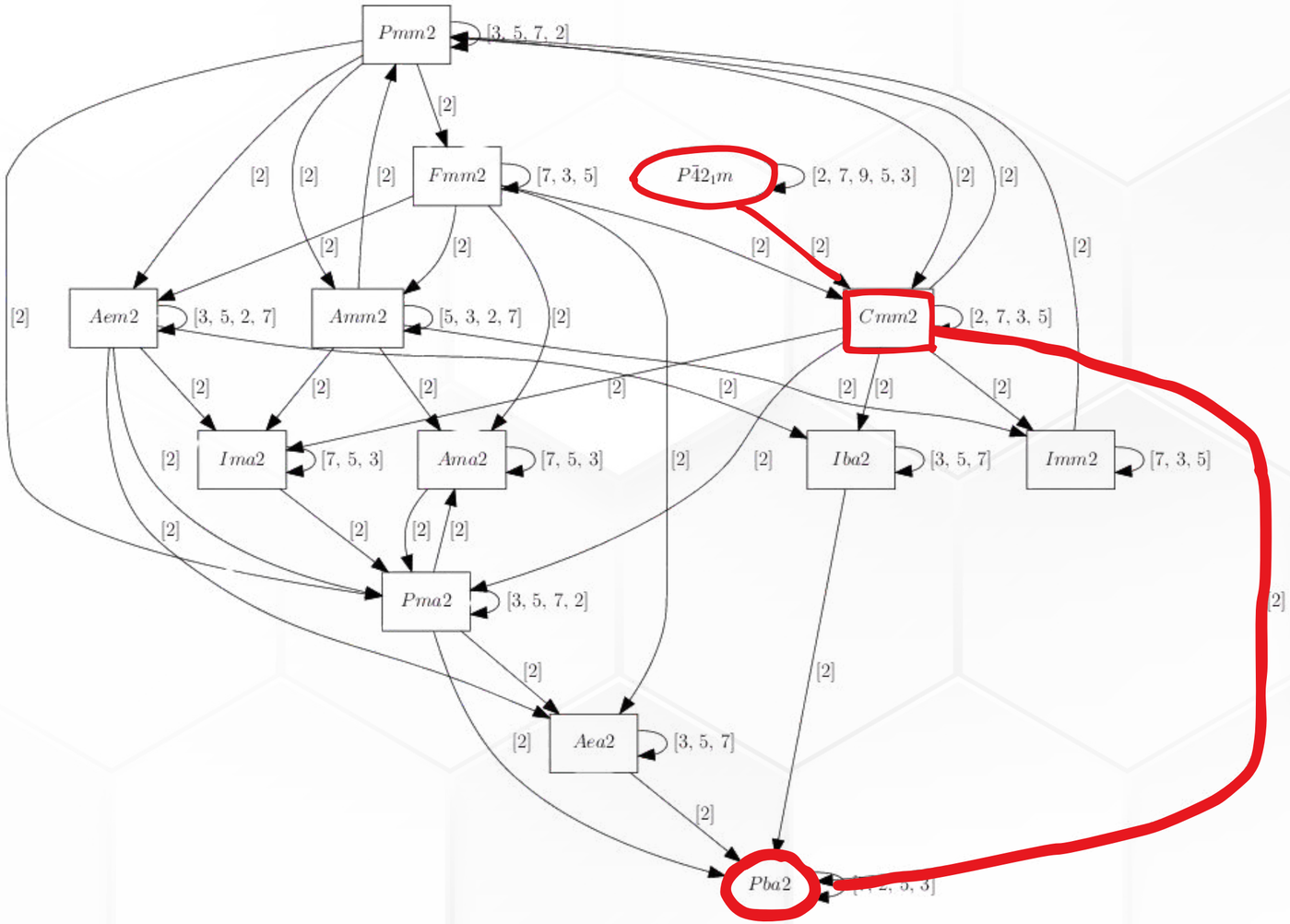

4. Fundamentals of Symmetry and Crystallography for Structural Analysis

Group–Subgroup & Amplimodes:

• Symmetry reduction G → S via translationengleich or klassengleich subgroups

• Amplimodes = time-frozen normal modes mapping high- to low-symmetry structures

• Amplitudes & polarization vectors quantify distortions driving phase transitions

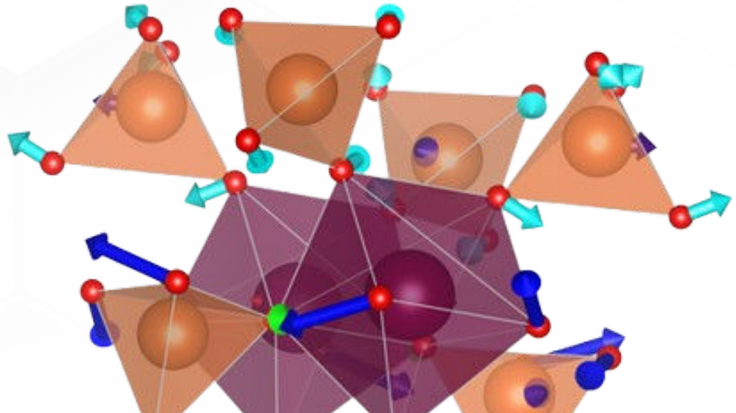

5. Transition β → β′, Main distortion modes (via amplimodes)

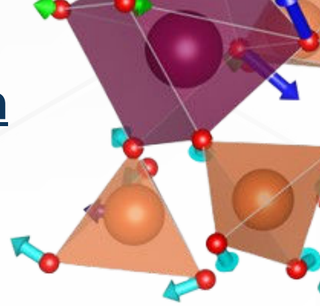

Transition to the β′ Phase (Ferroelastic & Improper Ferroelectric):

Tetragonal ($P\bar{4}2_1m$, Z=2) ⟶ Orthorhombic ($Pba2$, Z=4) with polar c-axis

- Group-subgroup transformation: not klassengleich nor translationengleich

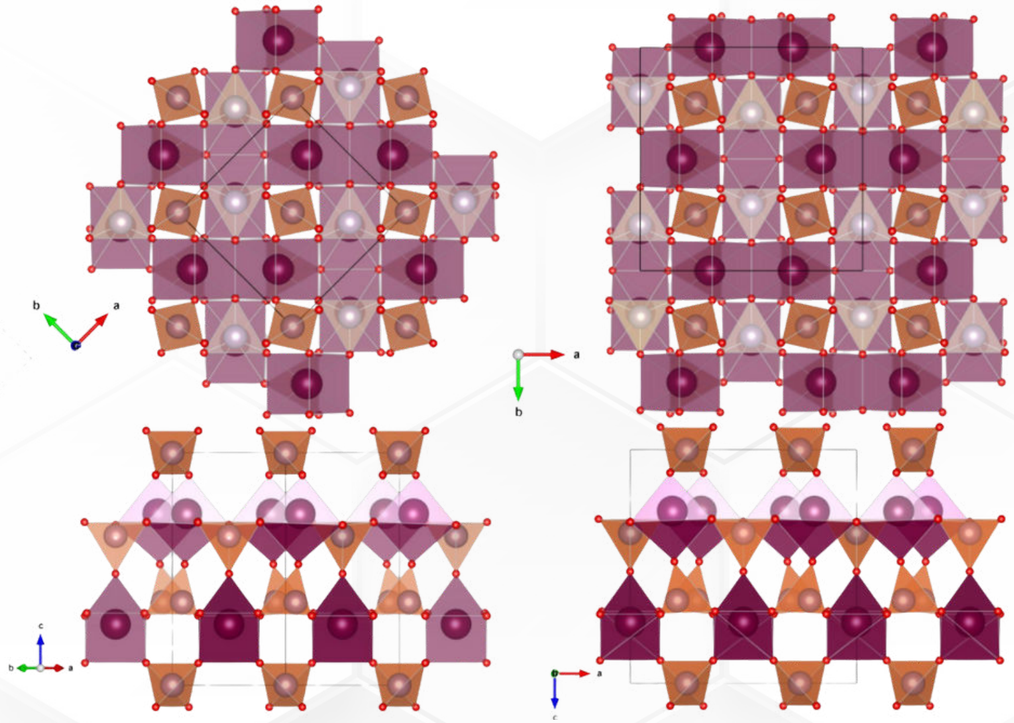

Improper ferroelectricity: polarization arises from coupled distortions.

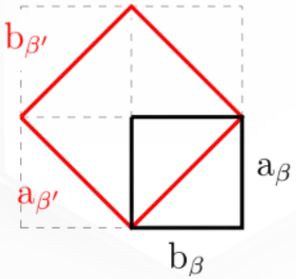

$$\mathbf{a}_{\beta'} = \mathbf{a}_\beta - \mathbf{b}_\beta$$
$$\mathbf{b}_{\beta'} = \mathbf{a}_\beta + \mathbf{b}_\beta$$
$$\mathbf{c}_{\beta'} = \mathbf{c}_\beta$$

$$\begin{pmatrix} \vec{a}' \\ \vec{b}' \\ \vec{c}' \end{pmatrix} = \underbrace{\begin{pmatrix} 0 & -1 & 0 \\ 1 & 1 & 0 \\ 0 & 0 & 1 \end{pmatrix}}_{A} \begin{pmatrix} \vec{a} \\ \vec{b} \\ \vec{c} \end{pmatrix}, \quad \vec{t} = \begin{pmatrix} 0 \\ \frac{1}{2} \\ 0 \end{pmatrix}$$

01 **Introduction**

5. Transition β → β′, Main distortion modes (via amplimodes)

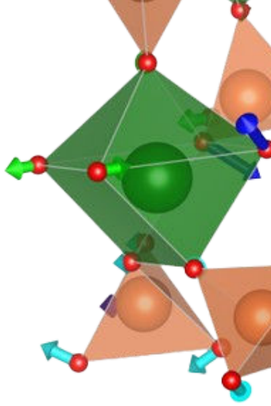

- **Main distortion modes (via amplimodes):**
  - Primary nonpolar: $M_2 \oplus M_4$ — breaks tetragonal symmetry
  - Secondary polar: Γ_3 — small displacements, induces polarization
  - Compatible symmetric mode: Γ_1 — does not reduce symmetry
- The primary mode dominates. Polar displacements along z are minimal → confirms improper ferroelectricity (polar mode is not the driving force).

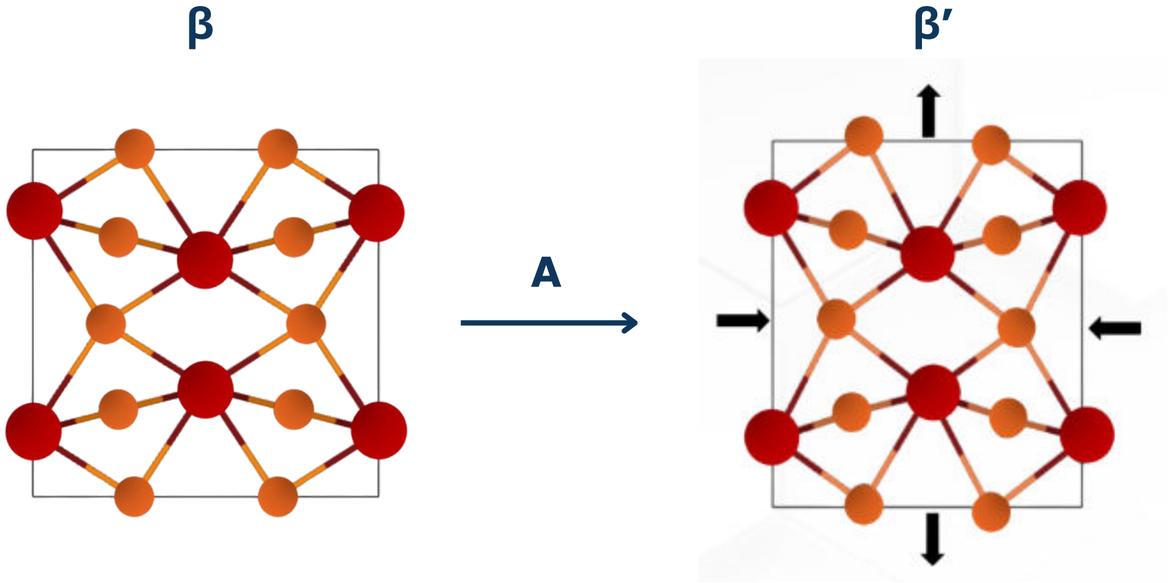

Ferroelastic strain:
tetragonal → orthorhombic transition

02 **Metodology I**

1. Synthesis of Rare-Earth Molybdates and Theoretical Calculations

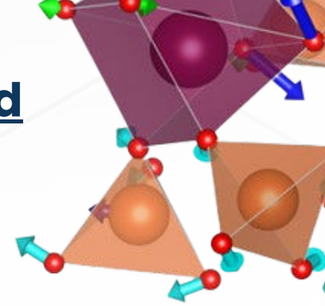

Synthesis of Rare-Earth Molybdates:

(a) (b) (c) (d)

(e) (f) (g)

Theoretical Calculations:

- DFT Overview: *Ab initio* method for many-electron systems, balancing accuracy and cost.
- ELSimMat Group (ULL): Expertise in crystal structures, electronic properties, and phonons; collaborates with CCDD.
- This Work: Uses VASP to compute β and β′ $Tb_2(MoO_4)_3$ structures – pseudopotentials + plane-wave basis.
- Procedure: For each volume, optimize atomic positions and lattice parameters under the original space-group constraints ($P\bar{4}2_1m$ for β; *Pba2* for β′) and Wyckoff sites.
- Goal: Provide theoretical benchmarks for experimental refinements and pressure-induced effects.

02 Metodology I

• Neutrons scatter from atomic nuclei and magnetic moments; X-rays scatter from electron clouds—making them complementary probes of atomic and magnetic structures.

• Two main interactions:

• Scattering: X-rays by electrons (form factor f(θ) ∝ Z, decreases at high angles); neutrons by nuclei (coherent length b_n independent of Z).
• Absorption: Photoelectric effect for X-rays (inner-shell capture → X-rays/Auger electrons); neutron capture → γ-emission or nuclear reactions.
• Cross-sections in barns (1 barn = 10^{-28} m^2) quantify interaction probabilities: coherent vs. incoherent scattering lengths for neutrons (fm scale).

• Elastic vs. inelastic processes:

• Elastic: no energy change → diffraction peaks (Bragg).
• Inelastic: energy exchange → phonons/magnons (neutrons) or Compton background (X-rays).

• Neutrons uniquely probe light atoms (O b_n ≈ 5.8 fm vs. Mo b_n ≈ 6.7 fm) and magnetism; no intensity loss at high angles.

• Incoherent neutron scattering arises from isotope variability and nuclear spin disorder (e.g. H vs. D).

• High neutron absorbers (Gd, Sm, Eu) degrade data—hence selection of Tb, Dy, Ho trimolybdates.

2. Radiation–Matter Interaction

Case of X-ray diffraction:

$$I_{hkl}(\mathrm{X}) \propto |F_{hkl}(\mathrm{X})|^2 \, L(\theta) \, P(\theta) \, A(\theta)$$

Where $F_{hkl}(X) = \sum_j f_j(\theta) \, e^{2\pi i(hx_j + ky_j + lz_j)}$ is the structure factor

(with $f_j(\theta)$ the atomic form factor of atom j)

Case of neutron diffraction:

$$I_{hkl}(n) \propto |F_{hkl}(n)|^2 \, L(\theta) \, A(\theta)$$

Where $F_{hkl}(n) = \sum_j b_j \, e^{2\pi i(hx_j + ky_j + lz_j)}$ is the neutron structure factor

(with b_j the nuclear scattering length of atom j)

3. Neutron and X-ray diffraction

3.1 Neutron generation and diffraction

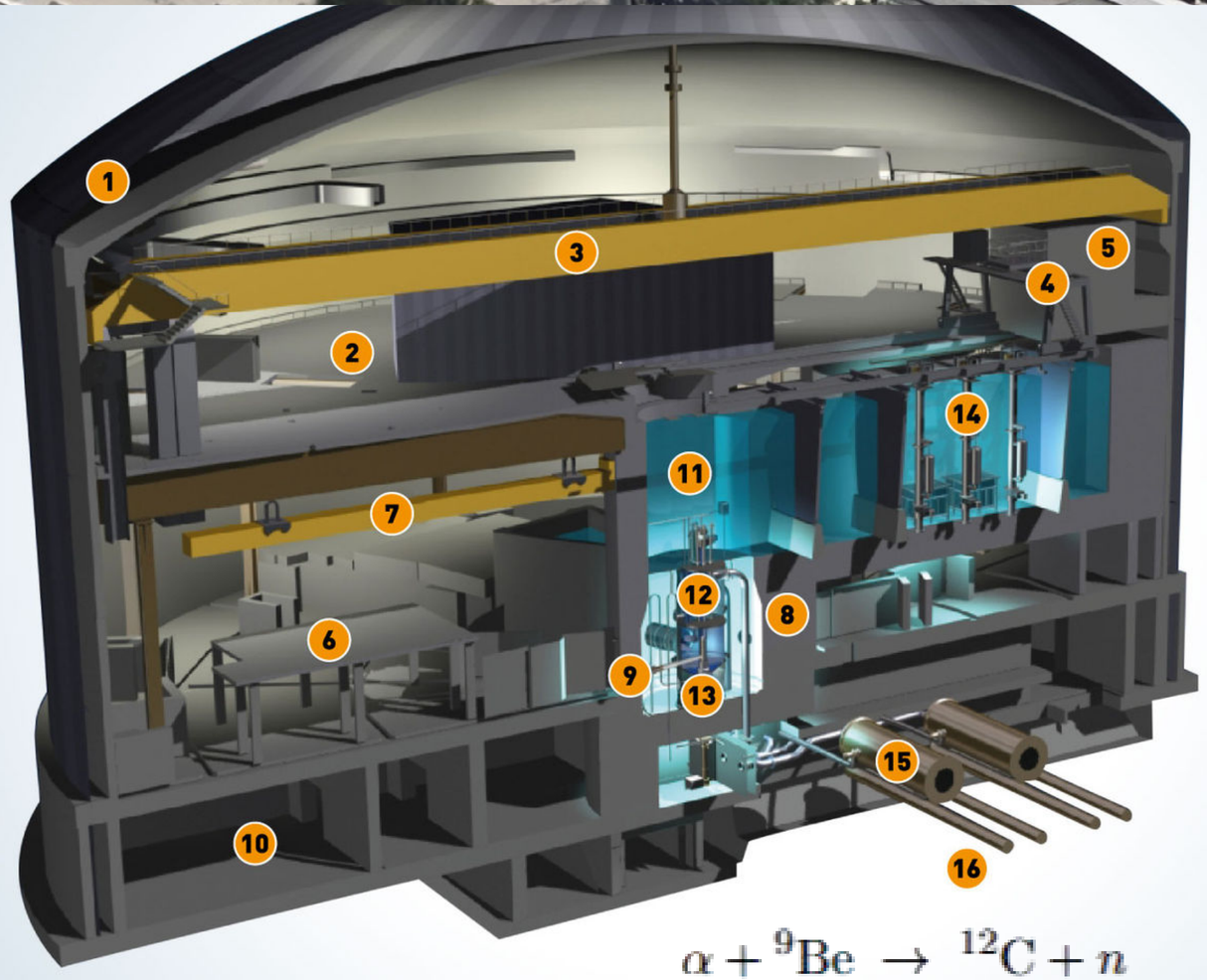

$$\alpha + {}^{9}\mathrm{Be} \rightarrow {}^{12}\mathrm{C} + n$$

1. Double-walled reactor building
2. Level D - reactor hall
3. Crane for reactor oerations level D
4. Gantry for handling of fuel elements
5. Hot cell
6. Level C - experimental hall
7. Crane for experimental operations
8. Biological shielding (concrete)
9. Collimated neutron exit point
10. Level B - reactor auxillary equipment
11. Reactor pool (light water)
12. Heavy water (moderator & fuel element cooling)
13. Fuel element
14. Spent fuel elements storage
15. Heat exhangers (primary/secondary)
16. Secondary cooling circuit 'drac river)

3. Neutron and X-ray diffraction

3.1 Neutron generation and diffraction

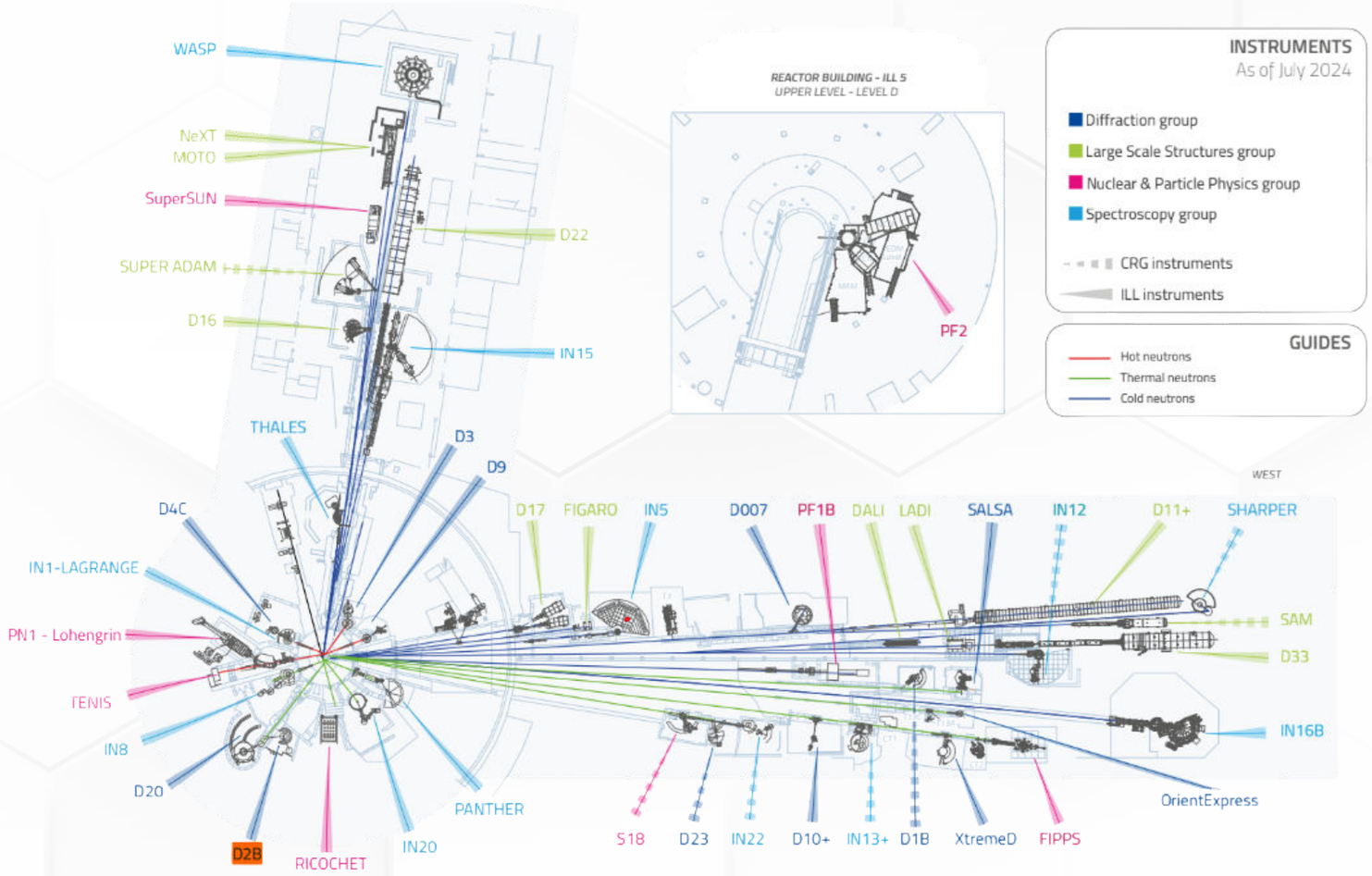

02 Metodology I

3. Neutron and X-ray diffraction

3.2 X-ray generation

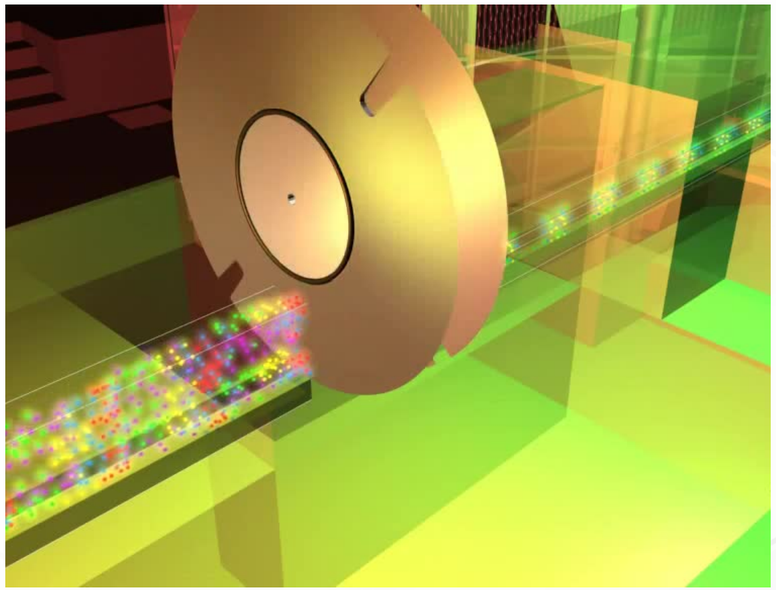

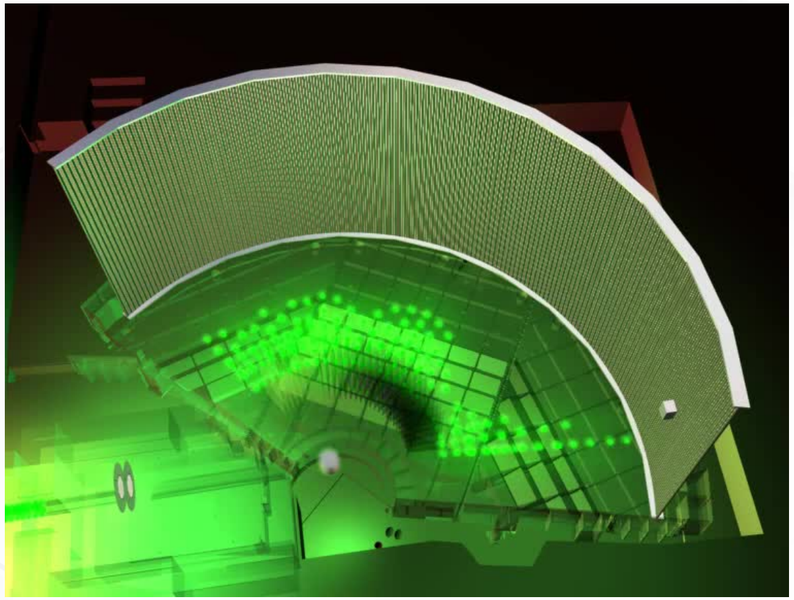

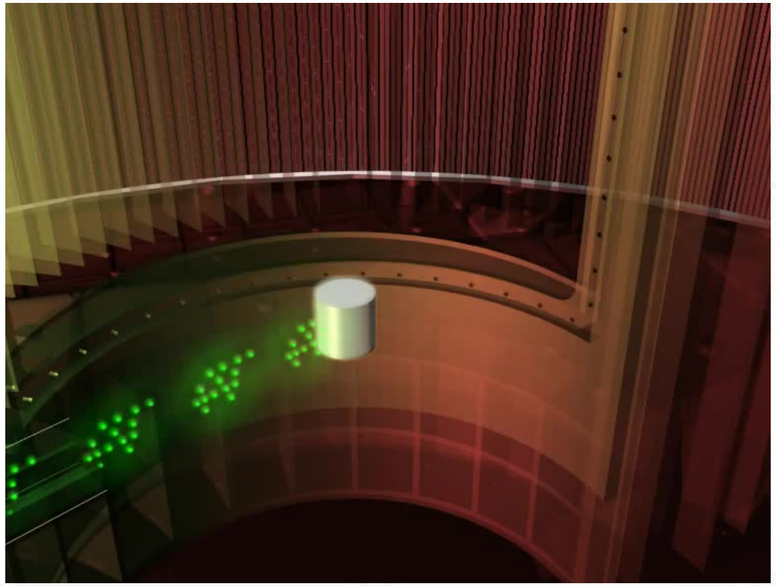

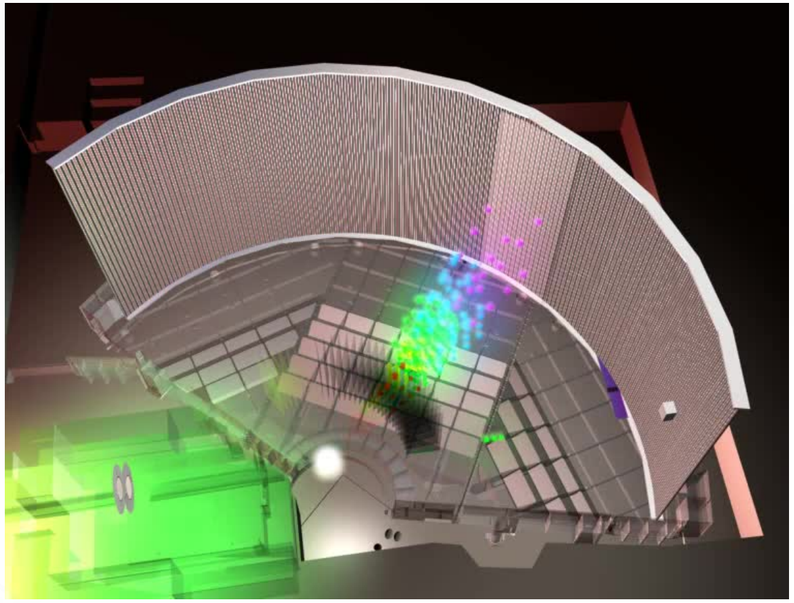

3. Neutron and X-ray diffraction

3.2 X-ray generation

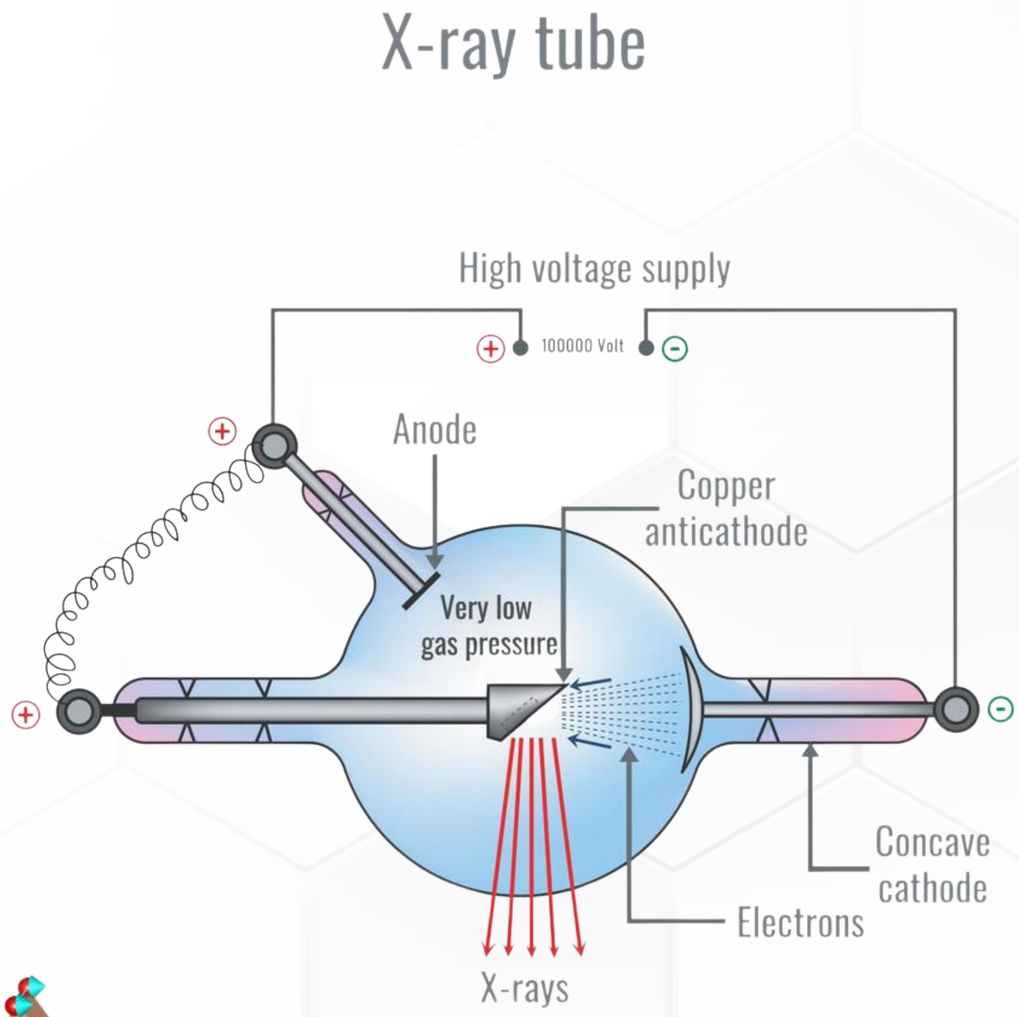

• X-ray Generation: Electrons from a heated filament are accelerated (30–45 kV) and collide with a copper anode.

• Characteristic Radiation: Inner-shell vacancies in Cu are filled → emit Cu Kα (λ = 1.5406 Å).

• Optimal Wavelength: Cu Kα balances angular range (5°–90° 2θ), resolution, and absorption.

• Beam Conditioning: Collimation and filtering remove Kβ and other unwanted lines for spectral purity.

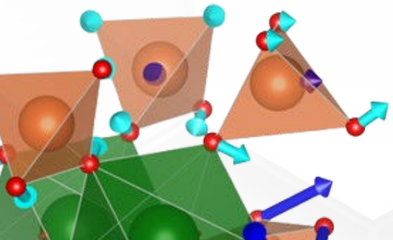

03 Metodology II

4. Powder Diffraction

- Powder Diffraction Principle: Uses randomly oriented microcrystals → all lattice planes satisfy Bragg's law simultaneously

- Data Extraction: Measure ring/band positions → determine θ → compute d_{hkl} via $n\lambda=2d_{hkl}\sin\theta$ → plot intensity vs. 2θ (diffractogram)

- Information Obtained: Phase identification, lattice parameters, crystallite size, texture, internal stresses

- Neutron Instrument (ILL D2B): Ge[335] monochromator (λ=1.5943 Å), 128 He^3 detectors (0–160°), high resolution & statistics, thermodiffraction capability

- X-Ray Instrument (PANalytical X'Pert PRO): Cu $K\alpha_1$ (λ=1.5405 Å), Bragg–Brentano geometry, divergence/anti-scatter/Soller slits, high-T chamber, reflection mode limitations (surface effects, texture, absorption)

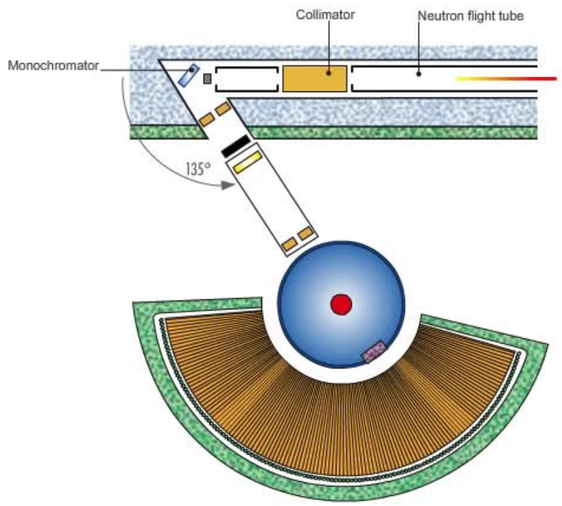

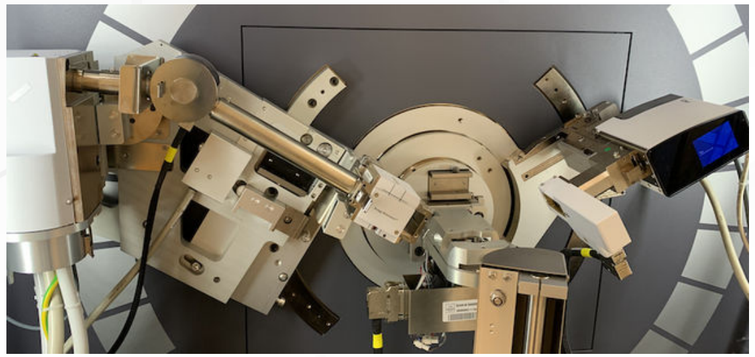

FullProf (WinPlotr)

Raw data

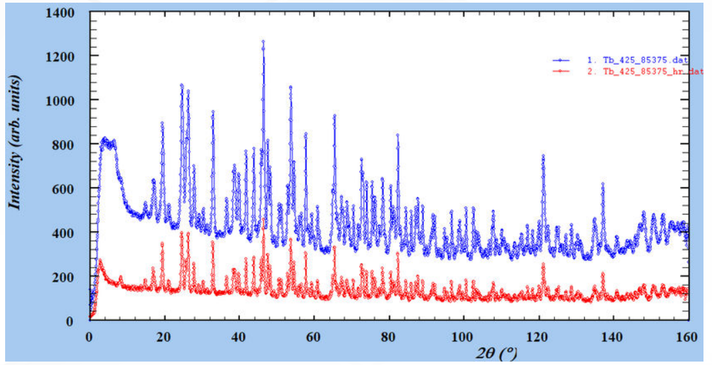

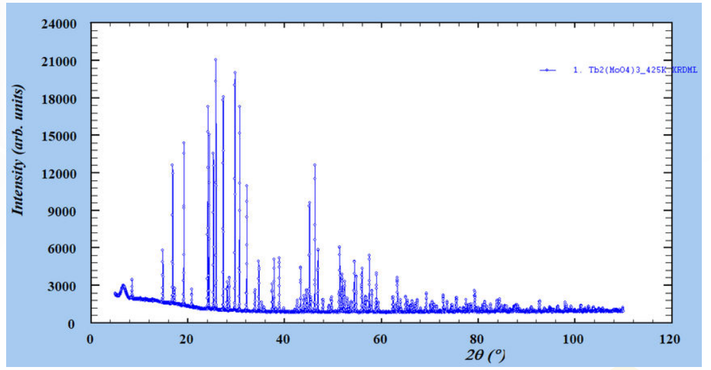

1. Introduction to Refinement

• Rietveld Method:
Least-squares fit of a theoretical diffraction model to experimental X-ray or neutron data by minimizing

$$S_y = \sum_i w_i \left(y_i^{\text{obs}} - y_i^{\text{calc}}\right)^2$$

• Model Ingredients:
Space group, atomic positions, thermal parameters

• Microstructure:
Crystallite size, microstrain, phase fractions

• Instrumental:
Peak broadening, optics effects

• Software:
FullProf multi-phase, multi-pattern refinement with shared parameters to reduce degrees of freedom

• **Calculated Intensity:**

$$Y_{i,c} = \sum_j Y_{i,j} = \sum_j S_j \sum_K L_{K,j}\, F_{K,j}^2\, \phi_{K,j}\left(2\theta_i - 2\theta_{K,j}\right) P_{K,j}\, A + y_{b,i}$$

- S_j ⟶ scale factor
- K_j ⟶ Bragg reflection for a given set of Miller indices.
- $L_{K,j}$ ⟶ correction factors such as Lorentz.
- $F_{K,j}^2$ ⟶ structure factor squared
- $\phi_{K,j}$ ⟶ peak profile function
- $P_{K,j}$ and A ⟶ profile and absorption corrections.
- $y_{b,i}$ ⟶ background intensity at point i.

1. Introduction to Refinement

Multipattern and Multiphase:

• Data Set: 9 patterns (6 neutron, 3 X-ray); 7 phases refined simultaneously (3 RE molybdates, Al, 3 Le Bail phases)

The **patterns** included in the refinements were:

- Pattern 1: Neutrons (full detector) of $Tb_2(MoO_4)_3$
- Pattern 2: Neutrons (detector center) of $Tb_2(MoO_4)_3$
- Pattern 3: X-rays of $Tb_2(MoO_4)_3$
- Pattern 4: Neutrons (full detector) of $Dy_2(MoO_4)_3$
- Pattern 5: Neutrons (detector center) of $Dy_2(MoO_4)_3$
- Pattern 6: X-rays of $Dy_2(MoO_4)_3$
- Pattern 7: Neutrons (full detector) of $Ho_2(MoO_4)_3$
- Pattern 8: Neutrons (detector center) of $Ho_2(MoO_4)_3$
- Pattern 9: X-rays of $Ho_2(MoO_4)_3$

The **phases** included in the refinements were:

- Phase 1: β-β′-$Tb_2(MoO_4)_3$
- Phase 2: β-β′-$Dy_2(MoO_4)_3$
- Phase 3: β-β′-$Ho_2(MoO_4)_3$
- Phase 4: β-β′-Aluminium
- Phase 5: Le Bail refinement of β-β′-$Tb_2(MoO_4)_3$
- Phase 6: Le Bail refinement of β-β′-$Dy_2(MoO_4)_3$
- Phase 7: Le Bail refinement of β-β′-$Ho_2(MoO_4)_3$

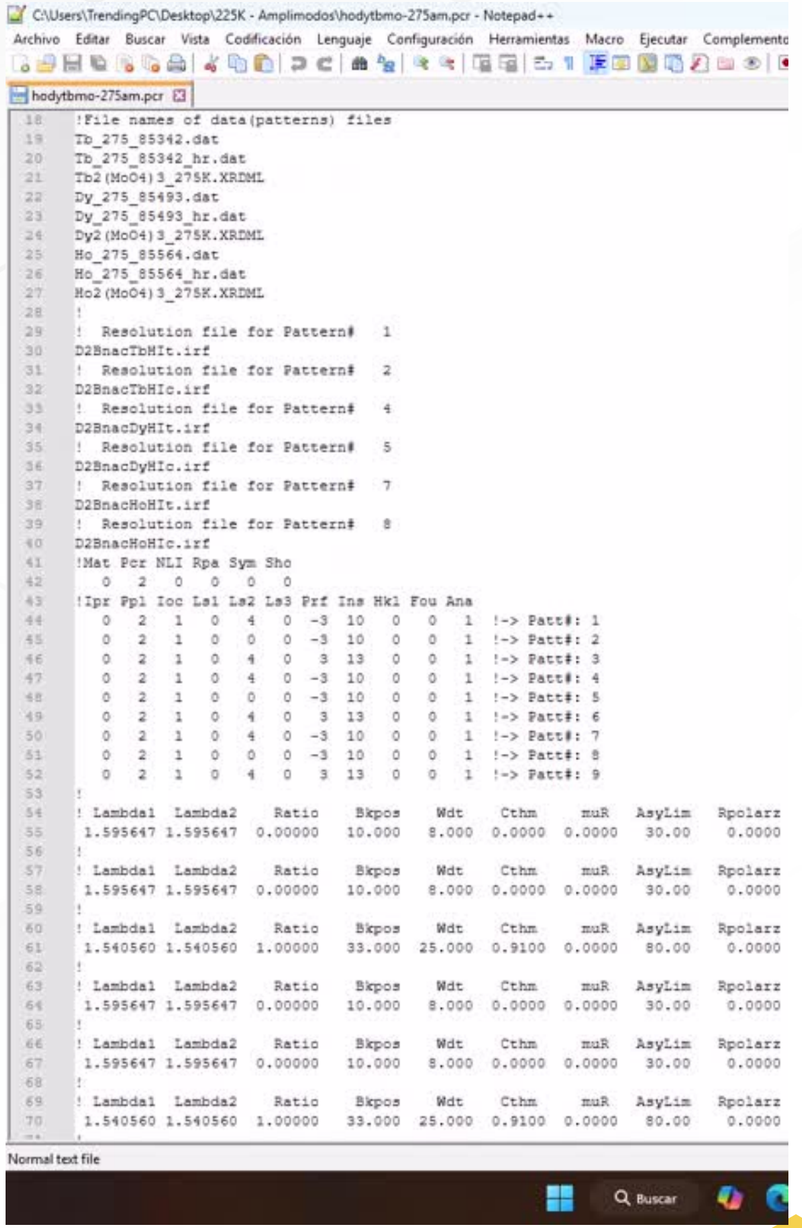

2. Modeling of the Diffraction Peak Profile in Rietveld Refinement

TCH Peak Profile: Pseudo-Voigt combining Gaussian + Lorentzian:

- $pV(x) = \eta L(x) + (1 - \eta)G(x)$, with mixing parameter η (0 = Gaussian; 1 = Lorentzian)
- $HG^2 = U \tan^2\theta + V \tan\theta + W$

Physical Parameters:

- U, V, W = instrumental Gaussian broadening
- X = crystallite size (Lorentzian)
- Y = microstrain (Lorentzian)

Asymmetry Correction:

- SL (tail intensity) & DL (tail decay)

Refinement Strategy:

- Neutrons: refine U, Y (negligible asymmetry)
- X-rays: refine U, V, W, X, SL, DL (axial divergence in low-angle tails)

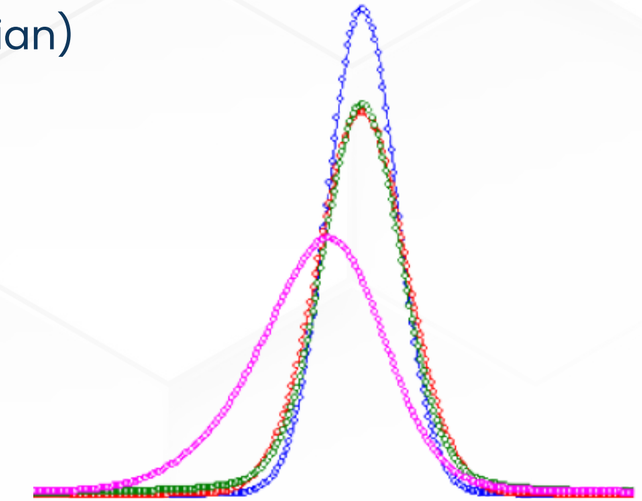

- **Instrumental Resolution Function: U, V, W (fixed parameters, neutrons) → blue**
- **Gaussian broadening (U, X-ray, neutrons) → red**
- **Lorentzian broadening (X, X-ray) → green**
- **Combining G and L + asymmetry → pink**

3. Background modeling in a diffraction pattern

• Background Role: Accounts for all non-Bragg scattering (fluorescence, incoherent scattering, noise, amorphous phases)

• Impact: Poor background fit distorts peak intensities → unreliable structural/microstructural parameters

• Approaches:
• Manual Points + Interpolation: User-defined intensities at selected 2θ → linear interpolate (early refinement)

• Global Functions: Simultaneously refine with structural parameters → continuous, reproducible baseline

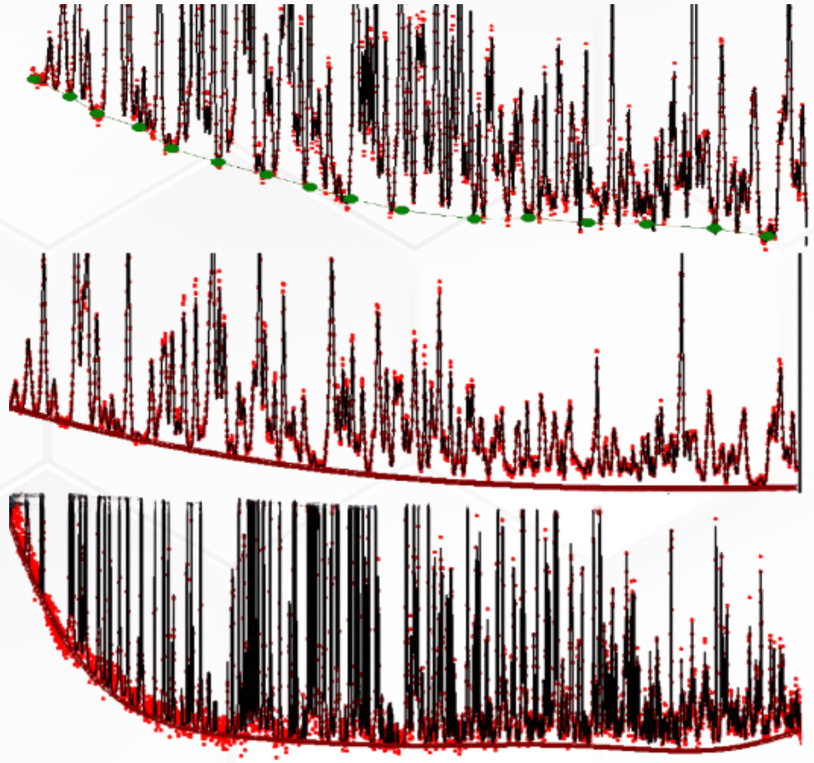

→ **Taylor**

→ **Chebyshev**

• **Neutron Data**:
• Taylor polynomials (m = 3) →
• Smooth, low-order fit ideal for gentle background trends

$$Y_{b,i} = \sum_{m=0}^{n} B_m \left(\frac{2\theta_i}{\mathrm{BKPOS}} - 1 \right)^m$$

• **X-ray Data**:
• Chebyshev polynomials (m = 9–11) →
• Orthogonal basis → stable, avoids artificial oscillations, captures local modulations

$$Y_{b,i} = \sum_{m=0}^{n} C_m \, T_m(x_i) \qquad x_i = 2 \, \frac{2\theta_i - 2\theta_{\min}}{2\theta_{\max} - 2\theta_{\min}} - 1$$

4. Treatment of Diffraction Intensities: Rietveld and Le Bail

• Rietveld Refinement:

• Fits full diffraction profile using a structural model
• Refines atomic positions, occupancies, thermal factors, microstructure & instrument

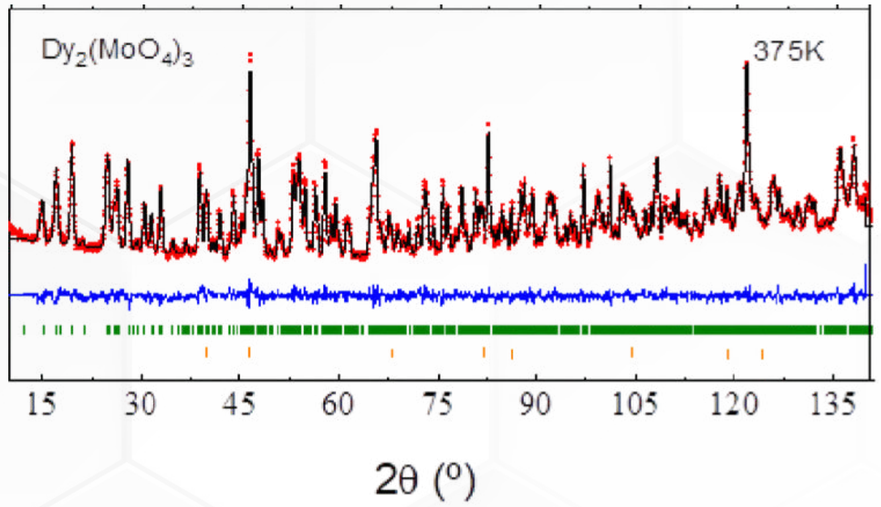

• Le Bail Refinement:

• Full-profile fit without atomic model
• Treats individual reflection intensities I_c(H) as refinable parameters
• Iterative update:

$$I_c^{(n+1)}(H) = I_c^{(n)}(H) \cdot \frac{\sum_i \left[\frac{y_o(2\theta_i) - y_b(2\theta_i)}{y_c(2\theta_i)}\right] \phi(2\theta_i - 2\theta_H)}{\sum_i \phi^2(2\theta_i - 2\theta_H)}$$

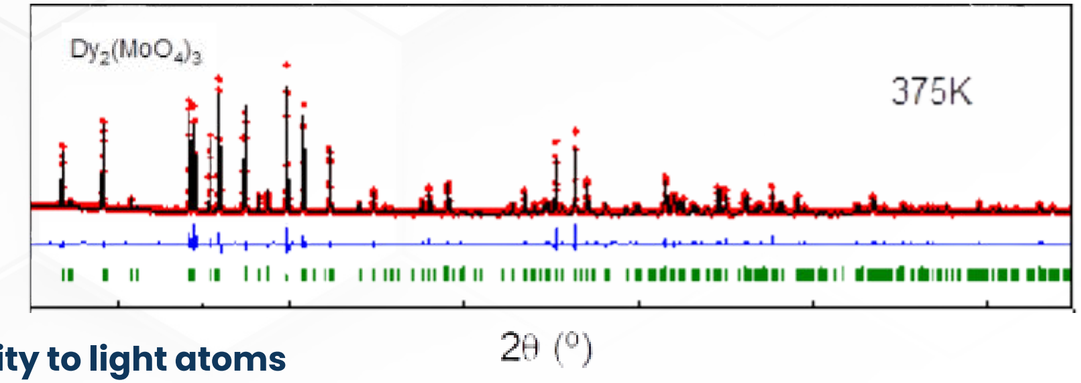

• **Ideal for X-ray data with preferred orientation, disordered phases, or low sensitivity to light atoms**

• **Combined Strategy:**
• **Neutrons: Rietveld → precise atomic structure (sensitive to light atoms, no texture)**
• **X-rays: Le Bail → accurate cell parameters & profile shapes when intensity model is unreliable**

03 Metodology II

5. *Amplimodes* in Structural Refinement

• Amplimodes Concepts:

• Collective atomic displacement modes tied to symmetry irreps, treated as “frozen” at t = 0
• Not time-dependent oscillations
• Static Distortion:

$$\mathbf{r}_i^{\mathrm{dist}} = \mathbf{r}_i^0 + \sum_m A_m \, \mathbf{p}_i^{(m)}.$$

• A_m: mode amplitudes $P_i^{(m)}$: polarization vectors

• Refinement Strategy:

• Refine A_m (few parameters) instead of 3N atomic coordinates

• Ensures symmetry compliance and avoids overfitting

• Advantages:

• Parameter Reduction → improved stability

• Physical Clarity → direct mode–distortion link

• Symmetry Enforcement → avoids incompatible distortions

• Transition Analysis → track mode amplitudes vs. T, P, etc.

• Group-Theory Link → systematic, reproducible comparisons

• Practical Implementation:

• Used AMPLIMODES (Bilbao) to get $P_i^{(m)}$ vectors

• In FullProf:

• Activated 3 mode sets for Tb/Dy/Ho:
Γ_1 (14 amps), Γ_3 (13 amps), $M_2^+ \oplus M_4$ (22 amps)
• Secondary modes set to zero above 425 K, then refined downwards

C:\Users\TrendingPC\Desktop\225K - Amplimodos\hodytbmo-275am.pcr - Notepad++

Archivo Editar Buscar Vista Codificación Lenguaje Configuración Herramientas Macro

hodytbmo-275am.pcr

```
O4_2    O         0.86669   0.17626   0.90250   0.00000   1.00000
                    0.00      0.00      0.00      0.00      0.00
          0.00391   0.00349   0.00155   0.00122 -0.00082  -0.00092
           751.00    761.00    771.00    781.00    791.00    801.00
O4_3    O         0.82375   0.36669   0.09750   0.00000   1.00000
                    0.00      0.00      0.00      0.00      0.00
          0.00391   0.00349   0.00155 -0.00122   0.00092  -0.00082
           751.00    761.00    771.00   -781.00   -801.00    791.00
O4_4    O         0.67625   0.13330   0.09750   0.00000   1.00000
                    0.00      0.00      0.00      0.00      0.00
          0.00391   0.00349   0.00155 -0.00122 -0.00092   0.00082
           751.00    761.00    771.00   -781.00    801.00   -791.00
! Polarisation Vectors of Symmetry Modes for each atom
V_MODES  147
! Nm  Atm     Irrep              Vx          Vy          Vz
   1  Tb1     GM1              0.000000    0.000000 -0.033289
   1  Tb1_2   GM1              0.000000    0.000000  0.033289
   2  Tb1     GM1             -0.033830    0.000000  0.000000
   2  Tb1_2   GM1              0.000000    0.033830  0.000000
   3  Mo2     GM1              0.000000    0.000000 -0.033289
   3  Mo2_2   GM1              0.000000    0.000000  0.033289
   4  Mo2     GM1             -0.033830    0.000000  0.000000
   4  Mo2_2   GM1              0.000000    0.033830  0.000000
   5  O1      GM1              0.000000    0.000000 -0.033289
   5  O1_2    GM1              0.000000    0.000000  0.033289
   6  O1      GM1             -0.033830    0.000000  0.000000
   6  O1_2    GM1              0.000000    0.033830  0.000000
   7  O2      GM1              0.000000    0.000000 -0.033289
   7  O2_2    GM1              0.000000    0.000000  0.033289
   8  O2      GM1             -0.033830    0.000000  0.000000
   8  O2_2    GM1              0.000000    0.033830  0.000000
   9  O3      GM1              0.000000    0.000000  0.023539
   9  O3_2    GM1              0.000000    0.000000  0.023539
   9  O3_3    GM1              0.000000    0.000000 -0.023539
   9  O3_4    GM1              0.000000    0.000000 -0.023539
  10  O3      GM1              0.016915    0.016915  0.000000
  10  O3_2    GM1             -0.016915   -0.016915  0.000000
  10  O3_3    GM1              0.016915   -0.016915  0.000000
  10  O3_4    GM1             -0.016915    0.016915  0.000000
  11  O3      GM1             -0.016915    0.016915  0.000000
  11  O3_2    GM1              0.016915   -0.016915  0.000000
  11  O3_3    GM1              0.016915    0.016915  0.000000
  11  O3_4    GM1             -0.016915   -0.016915  0.000000
  12  O4      GM1             -0.016915    0.016915  0.000000
  12  O4_2    GM1              0.016915   -0.016915  0.000000
  12  O4_3    GM1              0.016915    0.016915  0.000000
  12  O4_4    GM1             -0.016915   -0.016915  0.000000
  13  O4      GM1              0.000000    0.000000  0.023539
  13  O4_2    GM1              0.000000    0.000000  0.023539
  13  O4_3    GM1              0.000000    0.000000 -0.023539
  13  O4_4    GM1              0.000000    0.000000 -0.023539
  14  O4      GM1              0.016915    0.016915  0.000000
  14  O4_2    GM1             -0.016915   -0.016915  0.000000
```

Normal text file

6. Refinement Assessment

Visual Inspection First:

- **Overlay observed *vs.* calculated patterns to detect mismatches in peak shape, position, intensity, or background before relying on numerical values.**

Weighted profile R–factor:

$$R_{wp} = 100 \times \sqrt{\frac{\sum_i w_i \left(y_i^{\text{obs}} - y_i^{\text{calc}}\right)^2}{\sum_i w_i \left(y_i^{\text{obs}}\right)^2}}$$

Expected R–factor:

$$R_{\text{exp}} = 100 \times \sqrt{\frac{N - P}{\sum_i w_i \left(y_i^{\text{obs}}\right)^2}}$$

Reduced chi–square:

$$\chi^2 = \left(\frac{R_{wp}}{R_{\text{exp}}}\right)^2$$

Bragg R–factor:

$$R_{\text{Bragg}} = 100 \times \frac{\sum_k |I_k - I_k^{\text{calc}}|}{\sum_k |I_k|}$$

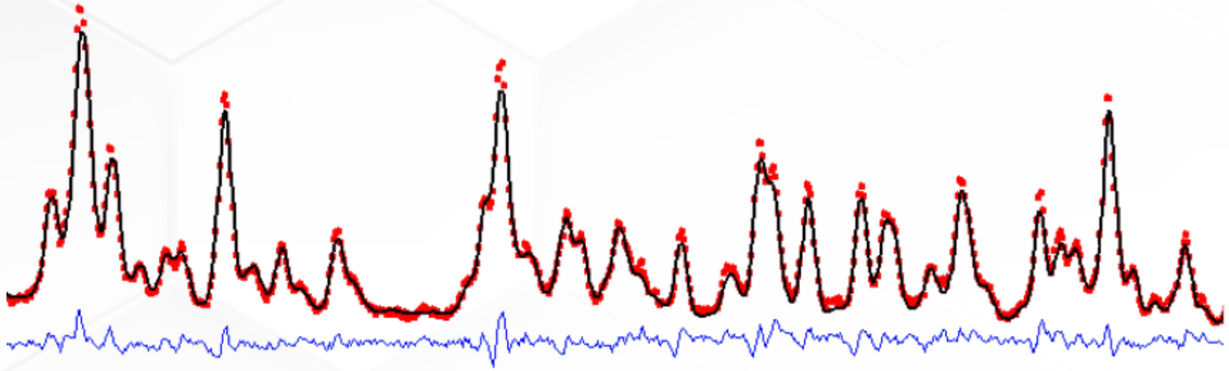

7. Refinement example in Fullprof

oad Edit PCR Mode Run Exit

```
=> Pattern:    6  Dy2(MoO4)3_425K
=> Pattern:    7  Ho_425_85597
=> Pattern:    8  Ho_425_85597_hr
=> Pattern:    9  Ho2(MoO4)3_425K
=> Ordering reflections contributing to each point for pattern:       1
=> Ordering reflections contributing to each point for pattern:       2
=> Ordering reflections contributing to each point for pattern:       3
=> Ordering reflections contributing to each point for pattern:       4
=> Ordering reflections contributing to each point for pattern:       5
=> Ordering reflections contributing to each point for pattern:       6
=> Ordering reflections contributing to each point for pattern:       7
=> Ordering reflections contributing to each point for pattern:       8
=> Ordering reflections contributing to each point for pattern:       9
=> Calculation of Yi for all points + Normal Matrix & Vector...
=> Calculation for pattern:       1
=> Calculation for pattern:       2
=> Calculation for pattern:       3
=> Calculation for pattern:       4
=> Calculation for pattern:       5
```


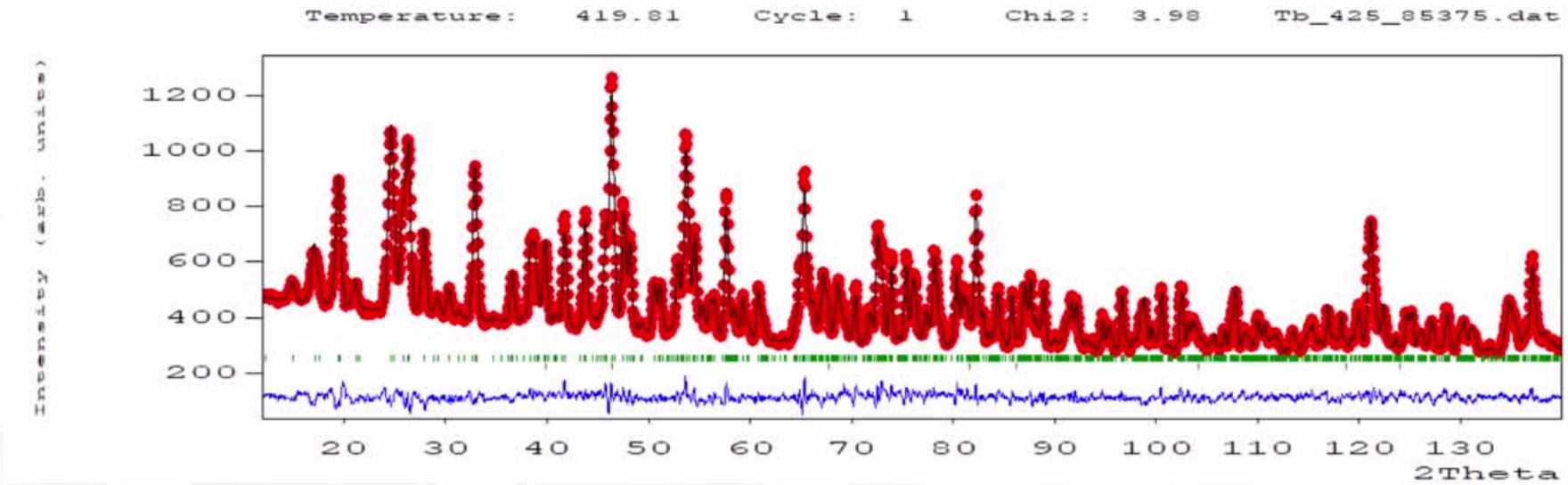

04 Analysis and Discussion of Results

1. Discussion of the X-ray Diffraction Patterns

$Tb_2(MoO_4)_3$

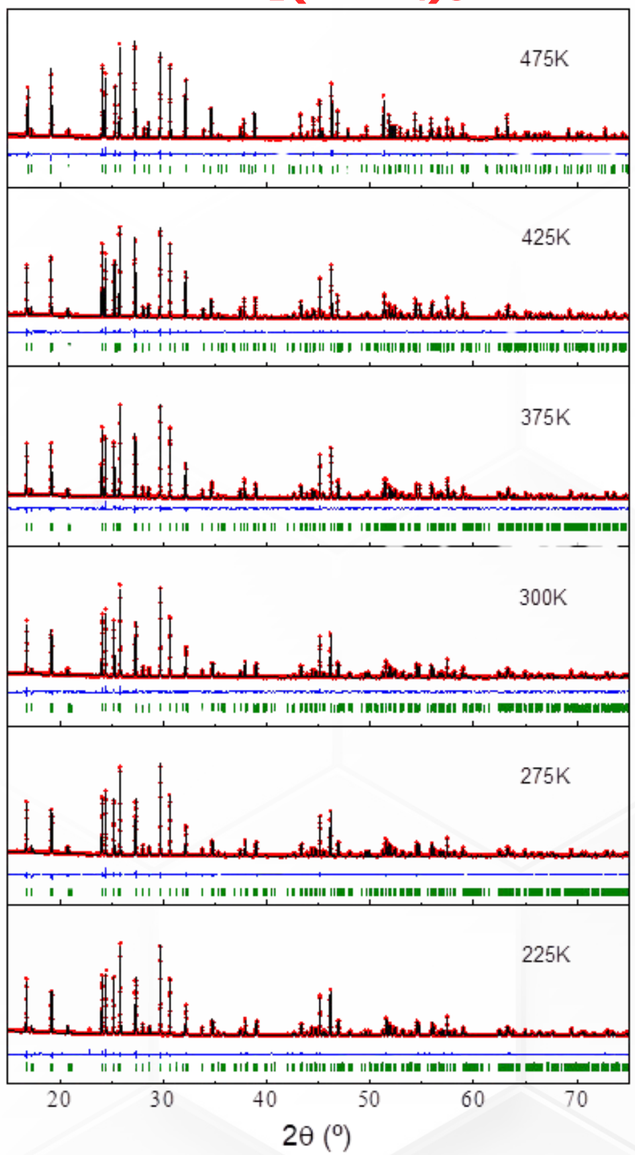

No significant peak shifts with T → minimal contraction by thermal or chemical pressure.

High-angle peaks show lower intensity due to the atomic form factor.

Parameter U (microstrain) ↓ with cooling, suggesting localized distortions before the phase transition.

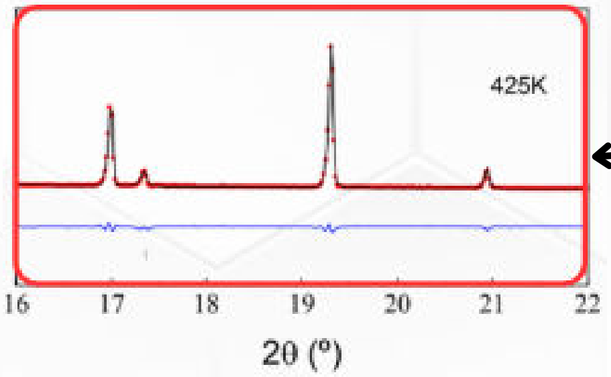

Ferroelectric peaks can be distinguished thanks to good peak separation and high data quality.

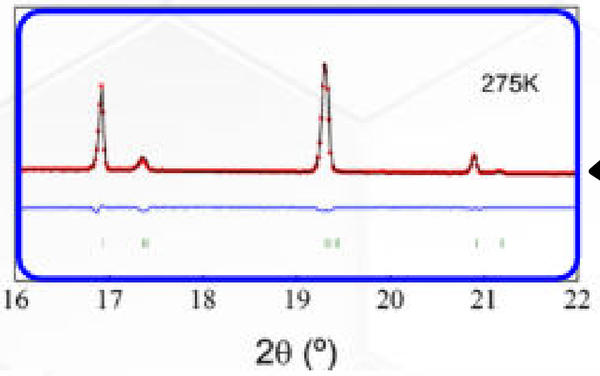

$Ho_2(MoO_4)_3$

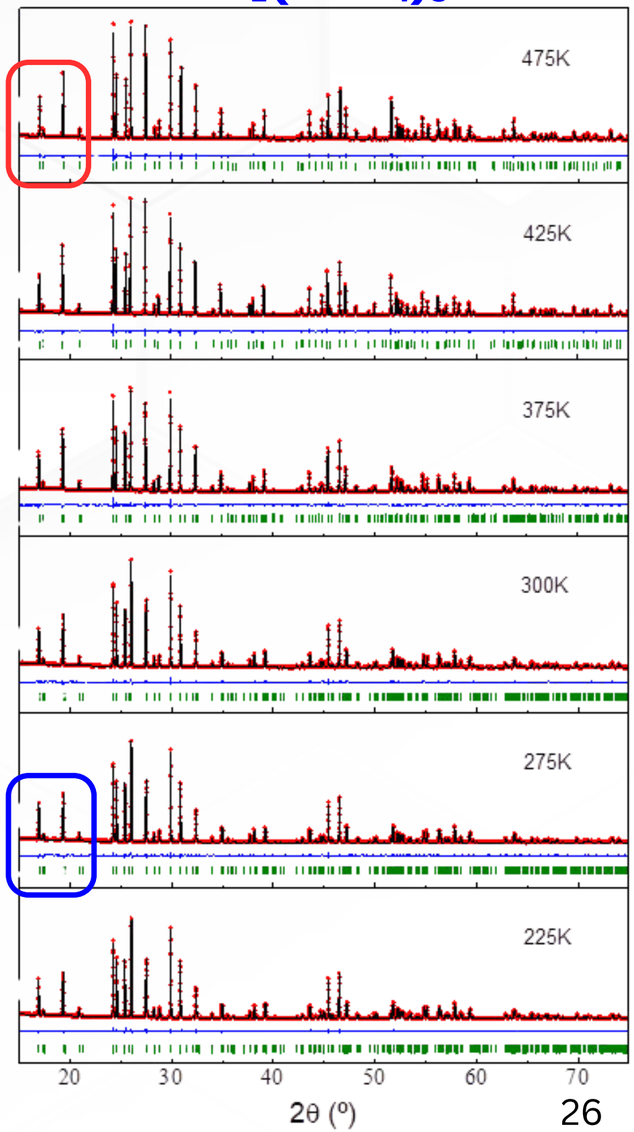

No atomic positions were refined — only profile data.

04 Analysis and Discussion of Results

2. Discussion of the neutron Diffraction Patterns

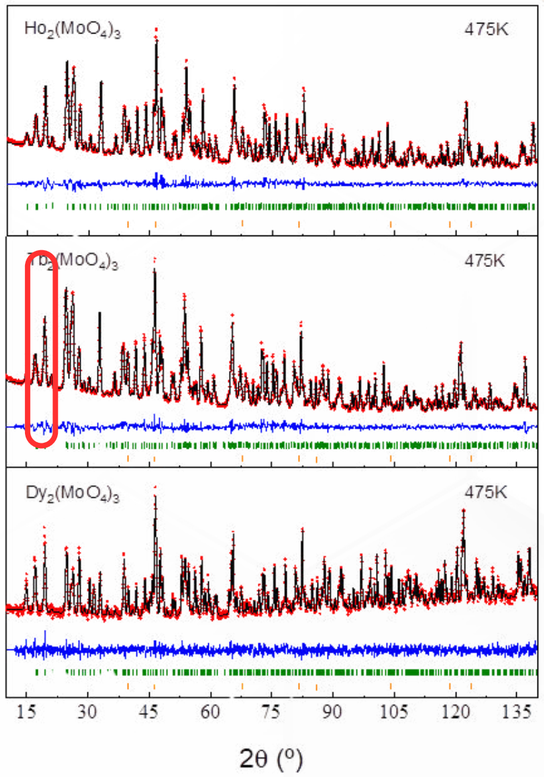

Excellent agreement between experimental and calculated profiles across all compounds and T.

Residuals are low, with accurate peak positions and good intensity fits, especially at low and medium angles.

Extra reflections from the aluminum sample holder were stabilized using multi-pattern refinement.

No clear peak shifts with decreasing temperature → minimal thermal or chemical pressure contraction.

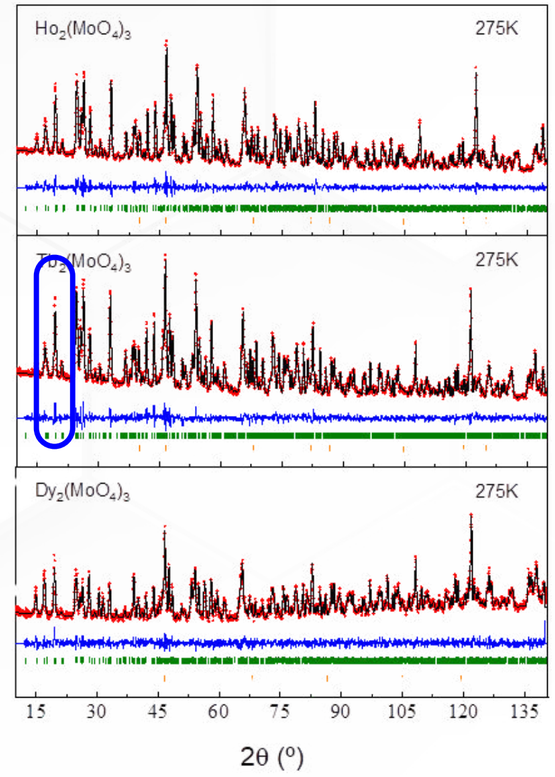

$Dy_2(MoO_4)_3$ shows lower quality due to high incoherent scattering and absorption → greater background noise and less defined peaks.

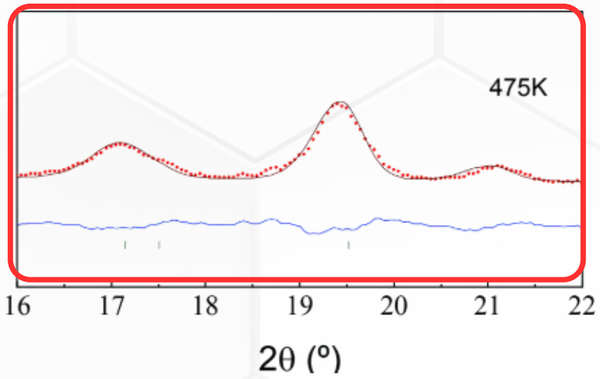

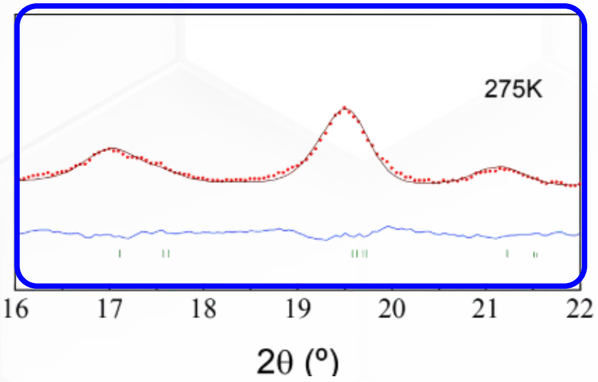

- **X-rays: U decreases with cooling (typical microstrain relaxation).**
- **Neutrons: U increases, likely due to reduced sensitivity to local distortions.**

3. Discussion of Cell Parameters, b-a. Differences, and Global *Amplimodes*

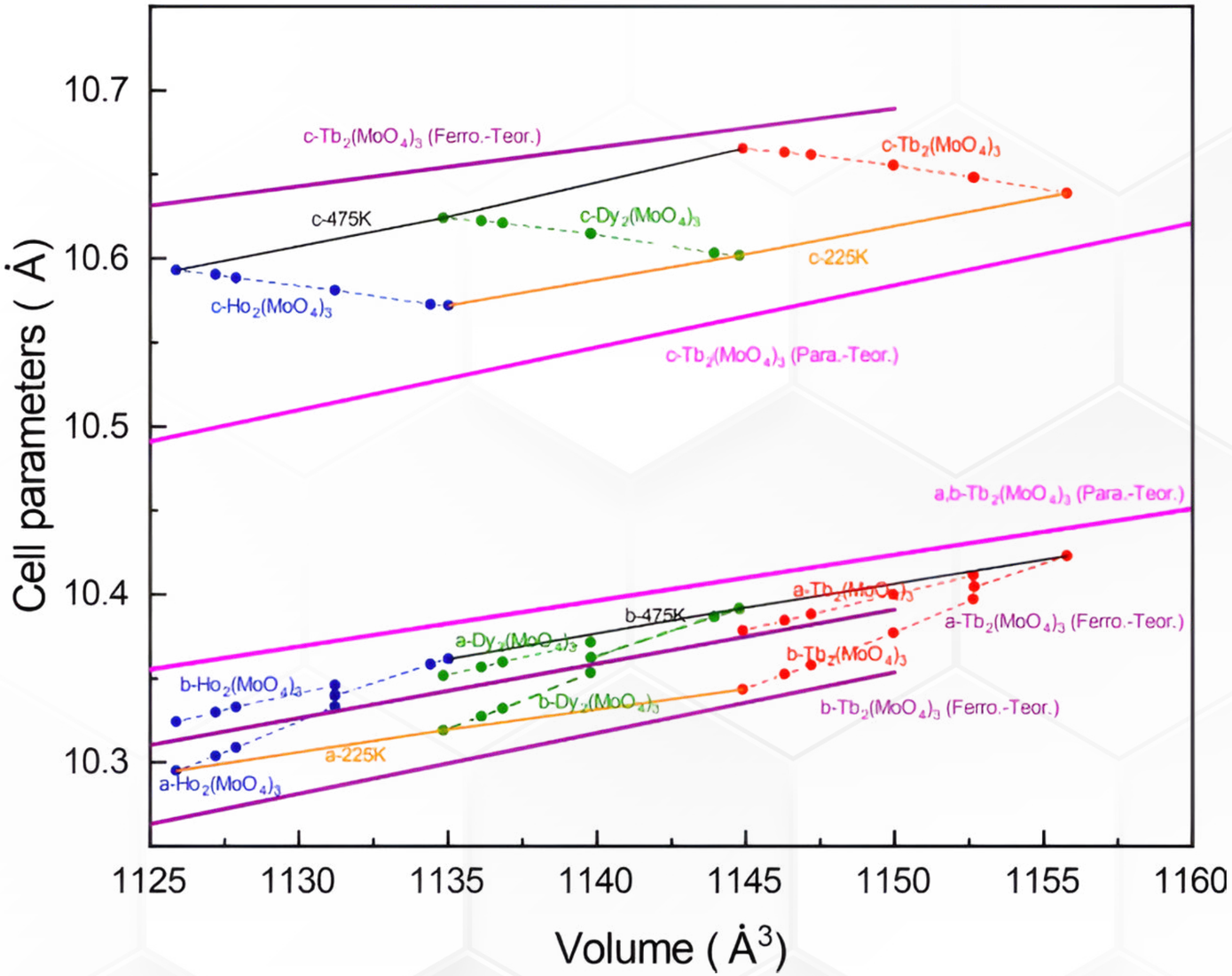

- **Coherence of contraction due to hydrostatic, chemical pressure and T**

- **Validity of theoretical models. General parameter contraction evolves from the theoretical paraelectric phase to the theoretical ferroelectric phase.**

- **Phase transitions:**
  - Detectable through discontinuities in a, b, and c parameters.

- **Approximate transition temperatures are identified.**

- **Cell parameters:**
  - **c** (polar axis) **↑ with ↓ T** (experimental); **↓ under pressure** (theoretical)
  - **a & b contract as V ↓** (experimental and theoretical).
  - In the paraelectric phase: a = b → tetragonal symmetry.

- **In the ferroelectric phase:**
  - Clear separation between a & b (b > a); more pronounced at lower volume (connects with figure below; this distortion is described by *amplimodes*).

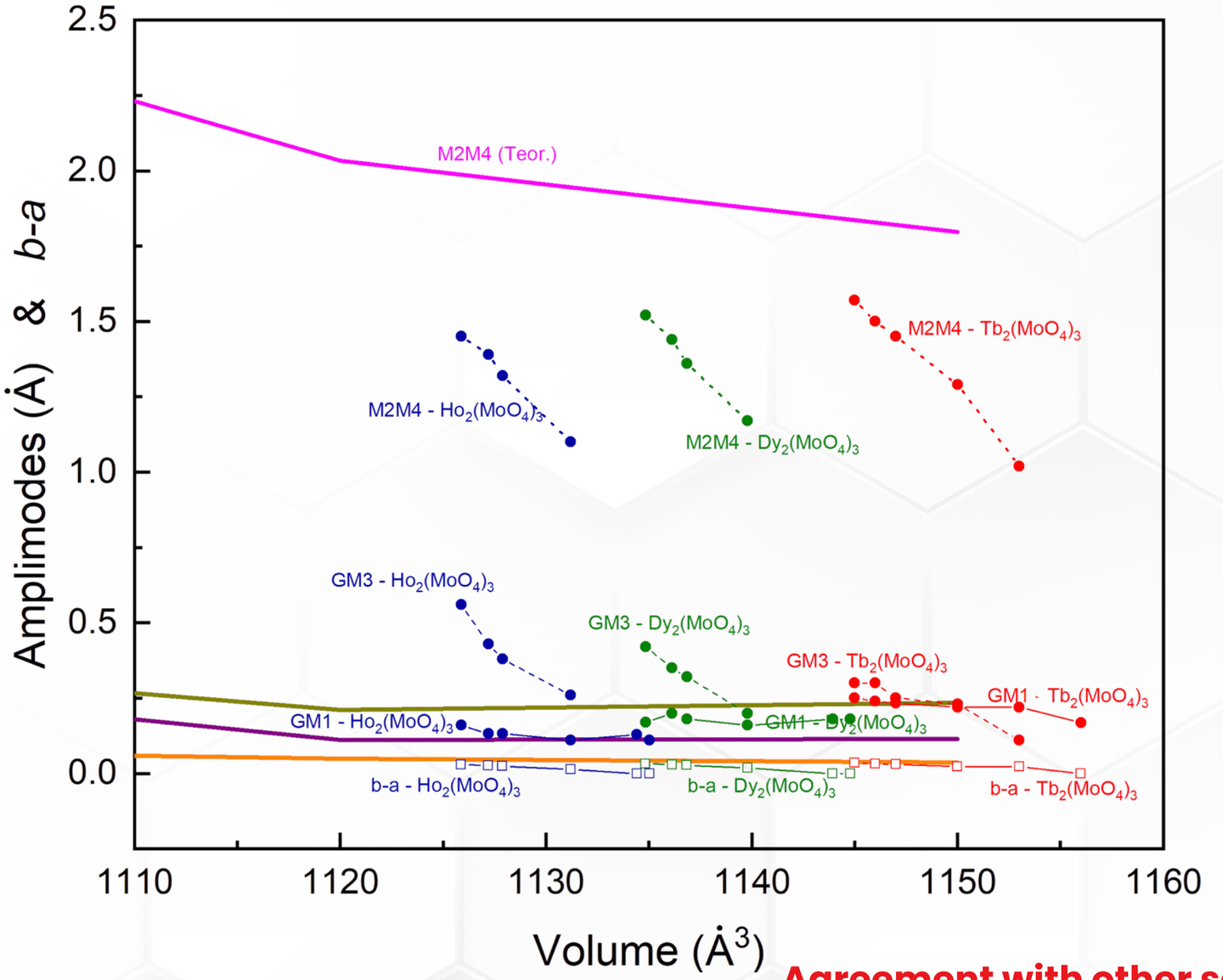

3. Discussion of Cell Parameters, b-a. Differences, and Global *Amplimodes*

• Parameter b – a:
- ↑ **with T** ↓ or applied pressure.
- ↓ with smaller ionic radius (though not monotonically).
- Represents the distortion seen in the previous graph (a–b separation).

• Primary mode $M_2^+ \oplus M_4$:
- Behavior similar to b–a.
- Larger amplitude than Γ_1 and Γ_3.
- Increases with ↓ volume (**↓ T or ↑ P**).
- **↓ with ionic radius** ↓ (Ho < Dy < Tb) → chemical pressure does not favor distortion.

• Mode Γ_3 (polar, responsible for polarization):
- **Increases with ↓ T and ↓ ionic radius.**
- For Dy & Ho: higher than Γ_1.
- For Tb: similar or lower than Γ_1.
- Concave behavior in theoretical calculations → possible complex structural coupling.

• Mode Γ_1 (non-polar):
- Not relevant in the transition → does not break symmetry.
- Depends on the chosen parent structure.

• Proposed:
- Extend calculations to Dy and Ho.

Agreement with other series ($La_xEr_{2-x}(MoO_4)_3$) supports these results

4. Individual *Amplimodes* and structural mechanisms

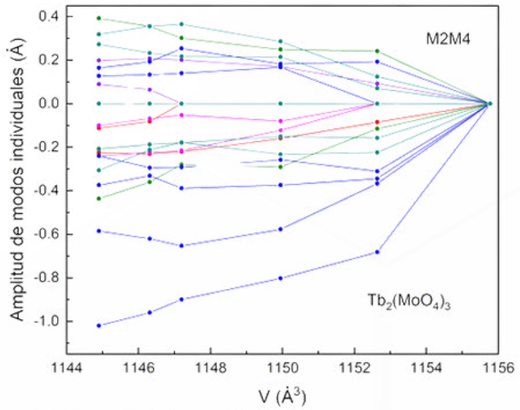

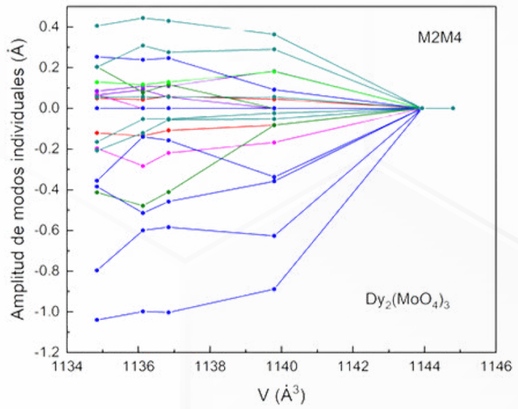

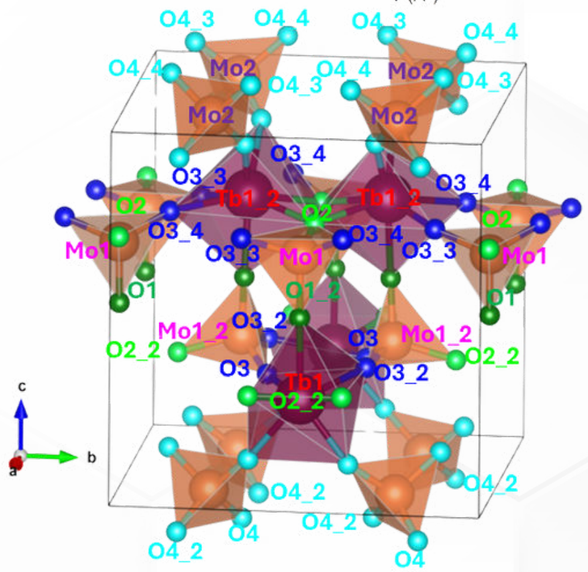

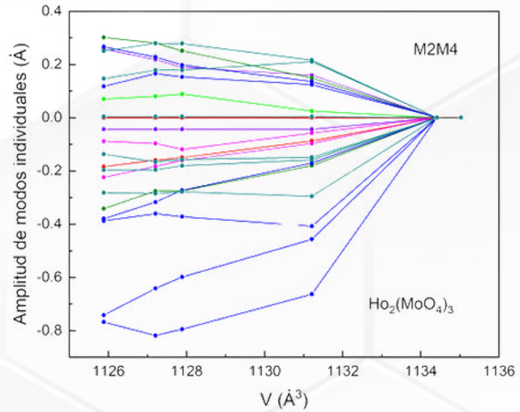

• Atoms in the ferroelectric structure have been colored according to the colors of the lines representing the evolution of the primary amplimode.

• Individual amplitudes of mode $M_2^+ \oplus M_4$ as a function of the unit cell volume.

• As temperature increases, the individual amplimodes generally elongate, in agreement with the behavior of the global amplimodes.
• As the ionic radius of the rare-earth increases:
• The individual displacements of the mode increase.
• A greater structural distortion is favored.
• A smaller ionic radius:
• Reduces the difference between tetrahedra and polyhedra.
• Restricts the movement of oxygen atoms.
• Acts as a chemical pressure that stabilizes the paraelectric phase.

• The smallest amplitudes are those associated with O2 (light green): minimal displacements, restricted due to their role as part of the dimer edge.

• The largest amplitudes are those associated with O3 (dark green/light blue): maximum displacements, in contrast with the previous ones, approximately located in the same plane.
The amplitudes of the heavy atoms are smaller, and the dark green and light blue oxygen atoms exhibit intermediate amplitudes.

4. Individual *Amplimodes* and structural mechanisms

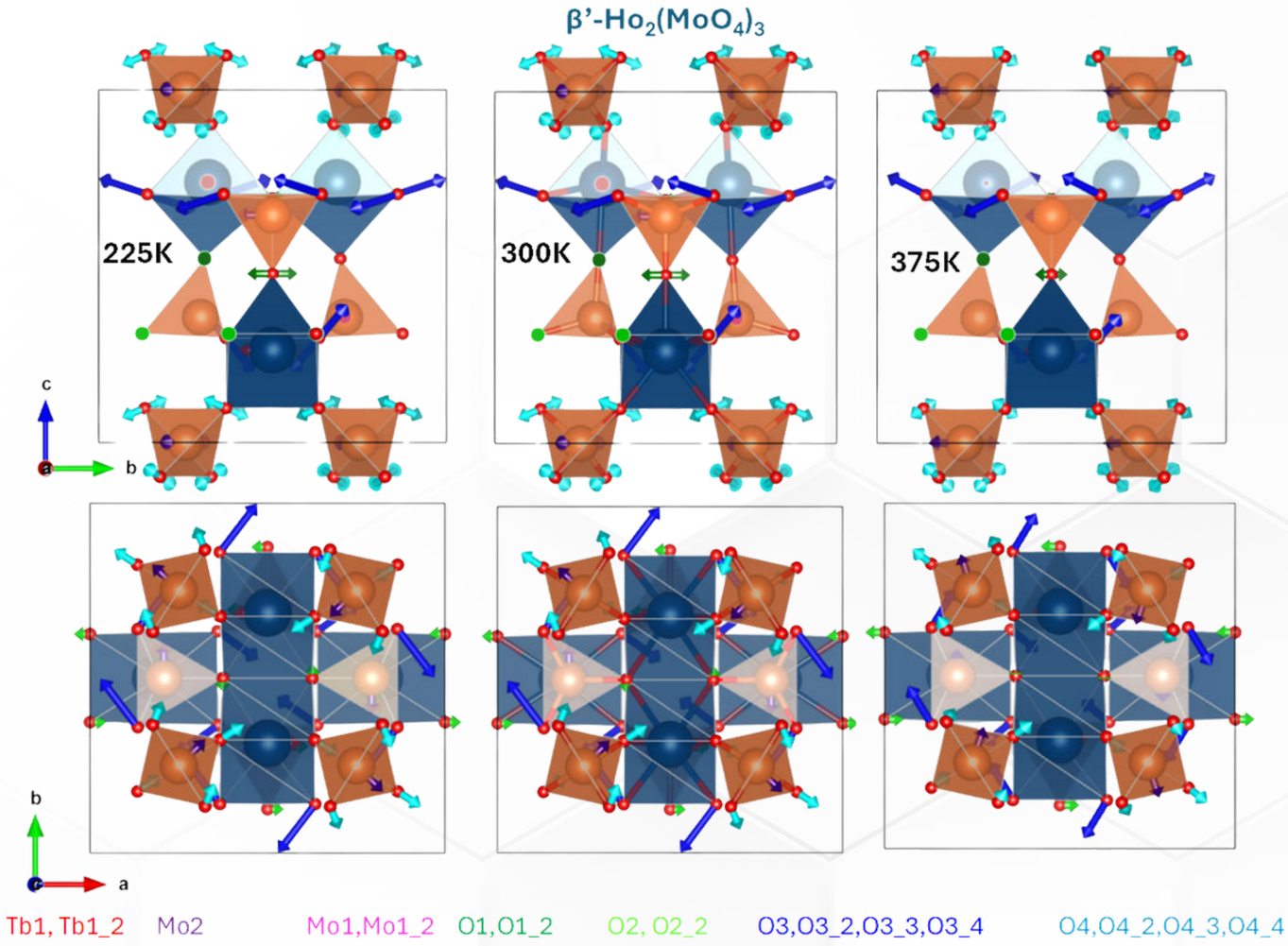

O2: small displacements perpendicular to the direction of the shared edge they belong to, with no significant changes with temperature.

O1: intermediate displacements in the diagonal direction of the ab plane (perpendicular to the Mo–O–Tb bridges along the c-axis). They increase as temperature decreases.

O4: intermediate displacements with three components, which rotate with temperature due to their greater freedom of movement.

O3: largest displacements with a strong component in the ab plane, which increase as temperature decreases. The c-axis component decreases with temperature.

- **Vectors indicate the atomic displacement when going from the paraelectric to the ferroelectric phase, compatible with the symmetry $M_2^+ \oplus M_4$. For better visualization, they have been multiplied by 5 (VESTA software).**

4. Individual *Amplimodes* and structural mechanisms

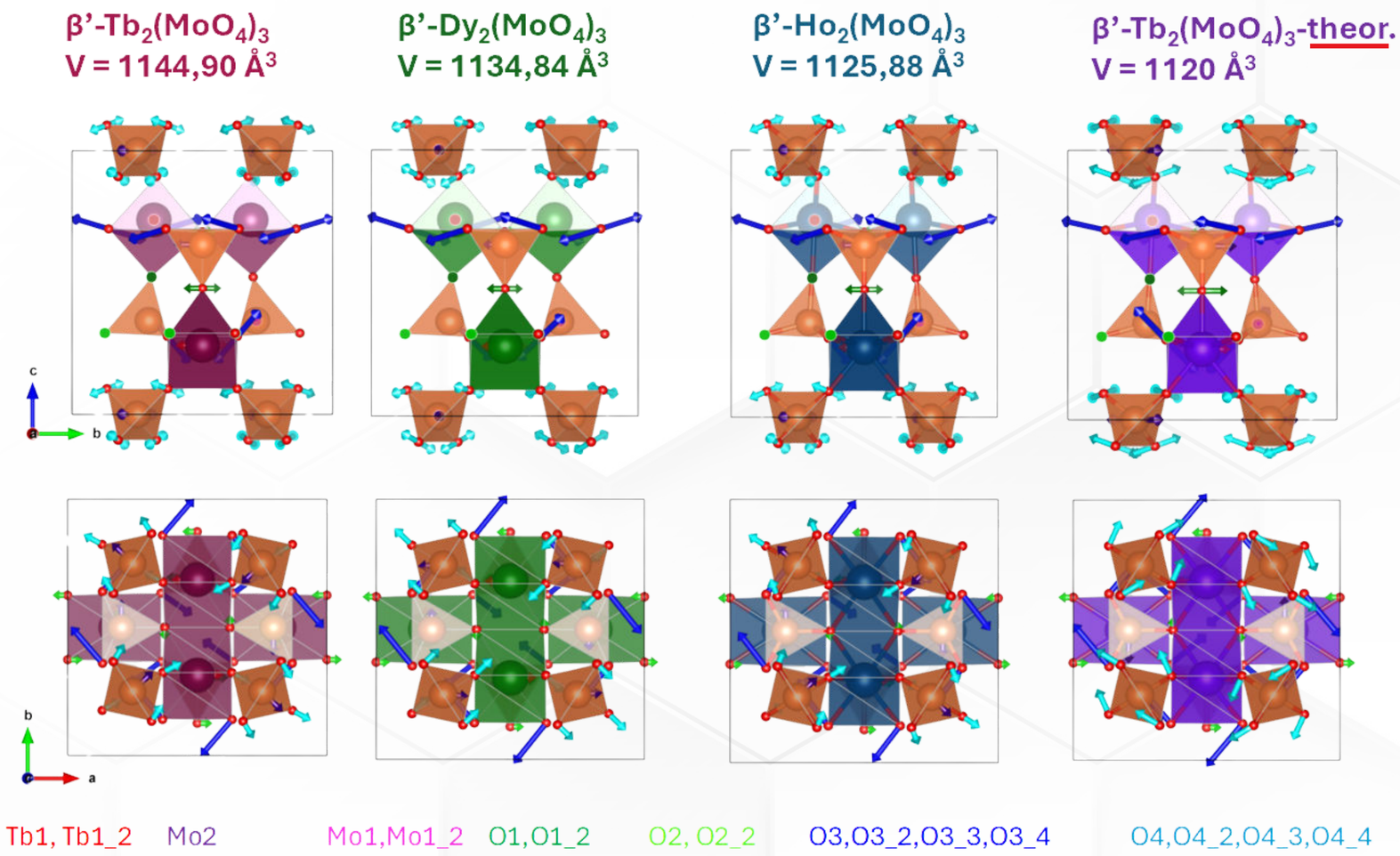

- Similar behavior is observed in the three compounds, which matches the theoretical results.
- The volumes of the represented structures are shown for better comparison.

- Vectorial displacements enlarged x50 for clearer representation

4. Individual *Amplimodes* and structural mechanisms

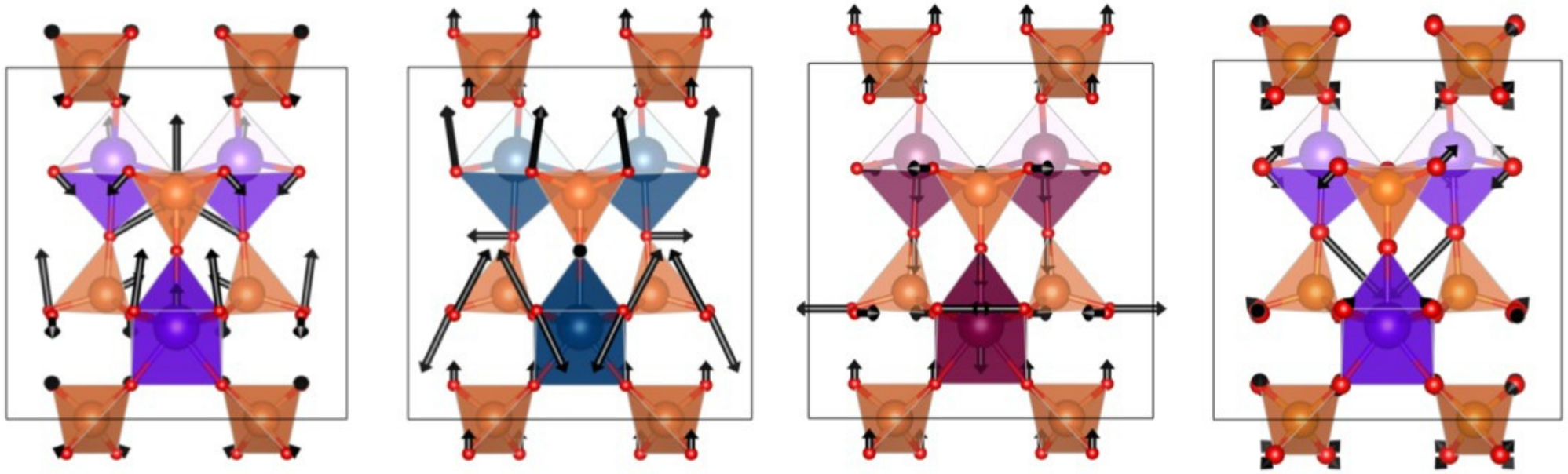

• Vectorial displacements enlarged x50 for clearer representation

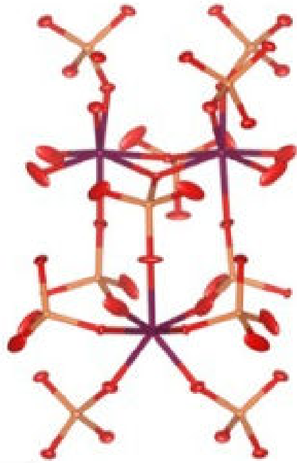

• Polar mode Γ_3 responsible for spontaneous polarization.

• Its amplitude increases as temperature decreases, and also increases with decreasing ionic radius.

• Its magnitude is about one order smaller than the primary mode and comparable to thermal displacements.
• This makes it difficult to extract firm conclusions from current refinements.

• Theoretical calculations show nonlinear dependence on volume for both Γ_1 and Γ_3.

• These modes exhibit energy minima and high sensitivity to small structural variations.
• Mode Γ_3 is activated not directly by volume changes, but through coupling with the primary mode and structural surroundings.

• This coupling enables complex phenomena in the ferroelectric transition.

05

Conclusions and Future Work

1. Conclusions

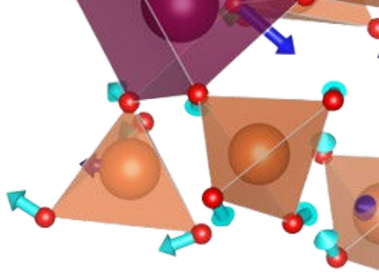

• Strategic material selection: Tb/Dy/Ho molybdates chosen for systematic comparison based on ionic radii and neutron absorption.

• Robust methodology: Combined X-ray & neutron multipattern refinements enabled accurate, coherent structural analysis.

• Amplimodes advantage: Enabled precise tracking of distortion modes linked to ferroelectric transitions, beyond atomic coordinate refinements.

• Thermal, chemical & pressure effects: Revealed consistent volume-dependent symmetry breaking and structural relaxation.

• Mode evolution:
• Primary mode ($M_2^+ \oplus M_4$) drives improper ferroelectric transition (↑ with decreasing volume).
• Secondary polar mode (Γ_3) shows nonlinear behavior, coupled to primary mode and structure.
• Ferroelectric complexity: Structural distortions depend on subtle interactions between symmetry modes and external variables—confirmed by experiments and theory.

05

Conclusions and Future Work

2. Future Work

• Structural analysis:
• Study bond lengths/angles to link atomic displacements with polyhedral distortions.

• Focus on oxygen bridges and coordination environments.
• Theoretical expansion:
• Extend DFT studies to Dy and Ho.
• Analyze less obvious secondary symmetry modes.

• Data correlations:
• Compute distortion indices for MoO_4 and REO_n groups.
• Relate them to $M_2^+ \oplus M_4$ and Γ_3 amplitudes.
• Add uncertainty bands for Γ_3 from grouped refinements.

• Advanced analysis tools:
• Use PCA/clustering on variables like mode amplitudes, *b-ab-ab-a*, ionic radius, volume.
• Overlay data from related compounds and visualize oxygen displacement vectors.

• Ferroelectric hysteresis:
• Measure loops at various temperatures in powders.
• Test if spontaneous polarization increases as ionic radius decreases (as seen in La_xEr_{2-x} series).
• Confirming this trend would allow tuning improper ferroelectricity via ionic size.

• Broader impact:
• Enable design of new functional materials with adjustable ferroelectric properties.

Universidad de La Laguna

Faculty of Sciences

05 Acknowledgements & Questions

THANK YOU

July 2025